

# PROJECT REPORT

On

**“SYNTHESIS, CHARACTERIZATION AND APPLICATION OF  
FLUORESCENT CARBON DOT FROM PRAWNS SHELL WASTE  
BY HYDROTHERMAL METHOD”**

Submitted by  
**ARYA NAIR**  
**AM20CHE004**

*In partial fulfillment for the award of the  
Post graduate Degree in Chemistry*



**DEPARTMENT OF CHEMISTRY  
AND  
CENTRE FOR RESEARCH**

**ST. TERESA'S COLLEGE (AUTONOMOUS)  
ERNAKULAM**

**2021-2022**

DEPARTMENT OF CHEMISTRY  
AND  
CENTRE FOR RESEARCH

ST. TERESA'S COLLEGE (AUTONOMOUS)  
ERNAKULAM



M.Sc. CHEMISTRY PROJECT REPORT

Name : ARYA NAIR  
Register Number : AM20CHE004  
Year of Work : 2021-2022

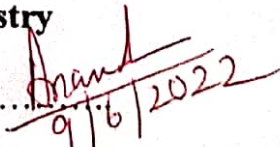
This is to certify that the project "SYNTHESIS, CHARACTERIZATION AND APPLICATION OF FLUORESCENT CARBON DOT FROM PRAWNS SHELL WASTE BY HYDROTHERMAL METHOD" is the work done by ARYA NAIR.

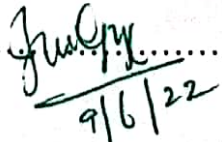
  
Dr. Jaya P. Varkey  
Head of the Department

  
Dr. Ushamani M  
Staff-member in charge

Submitted to the Examination of Master's degree in Chemistry

Date: 9/6/2022

Examiners: Dr. P. Ananthapadmanabhan   
9/6/2022

: Dr. Jenu George   
9/6/22

DEPARTMENT OF CHEMISTRY  
AND  
CENTRE FOR RESEARCH

ST. TERESA'S COLLEGE (AUTONOMOUS)  
ERNAKULAM



CERTIFICATE

This is to certify that the project work entitled "SYNTHESIS, CHARACTERIZATION AND APPLICATION OF FLUORESCENT CARBON DOT FROM PRAWNS SHELL WASTE BY HYDROTHERMAL METHOD" is the work done by ARYA NAIR under the guidance of Dr. Ushamani M, Associate professor, Department of Chemistry and Centre for Research, St. Teresa's College, Ernakulam in partial fulfilment for the award of the degree of Master of Science in Chemistry at St. Teresa's College, Ernakulam affiliated to Mahatma Gandhi University, Kottayam.

Dr. Ushamani M  
Project Guide  
Research Guide & Associate Professor  
Dept. of Chemistry & Centre for Research  
St. Teresa's College (Autonomous)  
Ernakulam

Dr. Jaya T. Varkey  
Head of the Department

DEPARTMENT OF CHEMISTRY  
AND  
CENTRE FOR RESEARCH


ST. TERESA'S COLLEGE (AUTONOMOUS)

ERNAKULAM



CERTIFICATE

This is to certify that the project work entitled "SYNTHESIS, CHARACTERIZATION AND APPLICATION OF FLUORESCENT CARBON DOT FROM PRAWNS SHELL WASTE BY HYDROTHERMAL METHOD" is the work done by ARYA NAIR under my guidance in the partial fulfilment for the award of the Degree of Master of Science in Chemistry at St. Teresa's College (Autonomous), Ernakulam affiliated to Mahatma Gandhi University, Kottayam.

  
Dr. Ushamani M  
Project Guide

Dr. Ushamani M.  
Research Guide & Associate Professor  
Dept. of Chemistry & Centre for Research  
St. Teresa's College (Autonomous)  
Ernakulam

## DECLARATION

I hereby declare that the project work entitled "SYNTHESIS, CHARACTERIZATION AND APPLICATION OF FLUORESCENT CARBON DOT FROM PRAWNS SHELL WASTE BY HYDROTHERMAL METHOD" submitted to Department of Chemistry and Centre for Research, St. Teresa's College (Autonomous) affiliated to Mahatma Gandhi University, Kottayam, Kerala is a record of an original work done by me under the guidance of Dr. Ushamani M , Associate professor, Department of Chemistry and Centre for Research, St. Teresa's College (Autonomous), Ernakulam. This project work is submitted in the partial fulfillment for the requirements for the award of the Degree of Master of Science in Chemistry.

  
ARYA NAIR

## *Acknowledgements*

---

First of all, I am highly grateful to Almighty God for his continuous blessings for the successful completion of my project.

I wish to express my profound sense of gratitude to Dr. Ushamani.M, my guide and Associate Professor of Department of Chemistry, St. Teresa's College for her valuable guidance, personal attention, meaningful suggestion, help and encouragement.

I take this opportunity to convey my gratefulness to Mrs.Sicily Rilu Joseph, Research scholar of Department of Chemistry, St. Teresa's College for the advice and help received from her.

I am also thankful to Dr. Jaya T Varkey, Head of the Department of Chemistry, St. Teresa's College, Ernakulam.

I would like to express my gratitude to all our teachers and non-teaching staff for the whole hearted help throughout my project.

I am grateful to the Principal Dr. Lizzy Mathew, St. Teresa's College, Ernakulam for being the pillars of support and providing good infrastructure for the study and development of students.

I thank Sophisticated Test and Instrumentation STIC, Cochin University & Technology, Kalamassery and the Department of Botany, St. Teresa's College, Ernakulam for the facilities provided for the analysis of my sample.

Last, but not the least, I am grateful to my loving family and friends for the care, support and concern they provide to follow my passion.

*Arya Nair*

Contents

<b>Chapter 1 INTRODUCTION</b>	13
<b>1.1 QUANTUM DOTS</b>	13
<b>1.2 CLASSIFICATION OF QUANTUM DOTS</b>	16
<b>1.3 CARBON QUANTUM DOTS</b>	18
<b>1.4 PROPERTIES OF CARBON DOT</b>	19
<b>1.5 APPLICATIONS PF CARBON DOTS</b>	24
<b>1.6 SYNTHESIS OF CARBON DOT</b>	27
1.6.1 TOP-DOWN APPROACH	28
1.6.2 BOTTOM-UP APPROACH	30
<b>1.7 SOURCES OF CARBON DOT</b>	36
1.7.1 CRUSTACEAN WASTE; AS A SOURCE OF CARBON DOT	38
<b>1.8 ANTIBACTERIALACTIVITY OF CARBON DOT</b>	40
<b>1.9 LITERATURE STUDY</b>	42
<b>1.10 OBJECTIVES OF THE WORK</b>	50
<b>Chapter 2 MATERIALS AND METHODS</b>	51
<b>2.1 CHARACTERIZATION TECHNIQUES</b>	51
2.1.1 FT-IR	51
2.1.2 UV-VISIBLE SPECTROSCOPY	52
2.1.3 TEM	53



2.1.4 XRD	54
2.1.5 SEM	55
2.1.6 EDAX	56
<b>2.2 SYNTHESIS OF CARBON DOT</b>	<b>57</b>
2.2.1 MATERIALS	58
2.2.2 METHOD	58
<b>2.3 SYNTHESIS OF ZINC OXIDE NANOPARTICLE FROM ZINC ACETATE</b>	<b>59</b>
2.3.1 MATERIALS	59
2.3.2 METHODS	60
<b>2.4 SYNTHESIS OF COPPER DOPED ZINC OXIDE NANOPARTICLE</b>	<b>60</b>
2.4.1 MATERIALS	60
2.4.2 METHOD	60
<b>Chapter 3 RESULTS AND DISCUSSION</b>	<b>62</b>
<b>3.1 CHARACTERIZATION OF CARBON DOT</b>	<b>62</b>
3.1.1 FT-IR STUDIES	62
3.1.2 UV-VISIBLE SPECTROSCOPY	63
3.1.3 FLUORESCENCE STUDY	64
3.1.4 TEM	65
<b>3.2 CHARACTERIZATION OF ZINC OXIDE NANOPARTICLES</b>	<b>67</b>
3.2.1 X-RAY DIFFRACTION	67
3.2.2 FT-IR STUDIES	70
3.2.3 SEM	72
3.2.4 EDAX	72
<b>3.3 CHARACTERIZATION OF COPPER DOPED ZINC OXIDE NANOPARTICLES</b>	<b>73</b>

3.3.1 X-RAY DIFFRACTION	73
3.3.2 FT-IR STUDIES	76
3.3.3 SEM	77
3.3.4 EDAX	78
<b>3.4 ANTIBACTERIAL STUDY OF CARBON DOT AND ITS NANOCOMPOSITE</b>	79
3.4.1 SYNTHESIS OF C-dot-ZnO NANOCOMPOSITE	79
3.4.2 SYNTHESIS OF C-dot-ZnO-Cu NANOCOMPOSITE	80
3.4.3 ANTIBACTERIAL ACTIVITY ASSAY	80
<b>Chapter 3 CONCLUSIONS</b>	83
4.1 CONCLUSIONS	83
<b>REFERENCES</b>	86

**LIST OF FIGURES**

Figure 1.1	Different synthetic methods of CD.
Figure 1.2	Autoclave reactor.
Figure 1.3	Different sources of CD.
Figure 2.1	Synthesized CD.
Figure 3.1	FT- IR spectra of synthesized CD.
Figure 3.2	UV-Vis spectra of synthesized CD.

Figure 3.3	Synthesized CD excited by UV light.
Figure 3.4	TEM images of synthesized CD.
Figure 3.5	XRD spectrum of zinc oxide nanoparticles.
Figure 3.6	FT-IR spectrum of zinc oxide nanoparticle.
Figure 3.7	SEM image of synthesized Zinc Oxide nanoparticles from Zinc Acetate.
Figure 3.8	EDAX spectrum of Zinc Oxide nanoparticles.
Figure 3.9	XRD spectrum of synthesized Copper doped Zinc Oxide nanoparticles.
Figure 3.10	FT-IR spectrum of synthesized Copper doped Zinc Oxide nanoparticles.
Figure 3.11	SEM image of synthesized Copper doped Zinc Oxide nanoparticles.
Figure 3.12	EDAX spectrum of synthesized Copper doped Zinc Oxide nanoparticles.
Figure 3.13	Images of <i>S. aureus</i> and <i>E. coli</i> bacteria after incubation.

<b>LIST OF TABLE</b>	
Table 3.1	FTIR peak assignments of Carbon dot.
Table 3.2	Average particle size of Zinc Oxide nanoparticles from Zinc Acetate.
Table 3.3	FTIR peak assignments of Zinc Oxide nanoparticles from Zinc Acetate.
Table 3.4	Average particle size of copper doped Zinc Oxide nanoparticles.
Table 3.5	FTIR peak assignments of Copper doped Zinc Oxide nanoparticles.
Table 3.6	comparison of antibacterial activity

<b>LIST OF ABBREVIATIONS</b>	
Quantum dot	QD
Carbon dot	CD
Graphene quantum dot	GQD
Photoluminescence	PL
Transmission electron microscopy	TEM
Fourier transform infrared spectroscopy	FT-IR
Attenuated total reflection	ATR
UV-Visible spectroscopy	UV-Vis
X-ray diffraction	XRD
Scanning electron microscope	SEM
Energy dispersive x-ray analysis	EDAX

# Chapter 1

## **INTRODUCTION**

### **1.1 QUANTUM DOTS**

Quantum dots are semiconductor nanoparticles having size range of 2–10 nm. They are materials showing quantum confinement effects in all dimensions. It was first synthesized in a glass matrix by Alexey Ekimov in 1981 and in colloidal suspension by Louis Brus in 1983[1]. They were first theorized by Alexander Efros in 1982 with the aim of explaining the behaviour of these very small crystals by the confinement of their electron. In Europe, it is Arnim Henglein, German chemist who paved the way to Quantum Dots in Berlin since 1982. In Asia, Tadashi Itoh at Sendai in Japan started to work on CuCl Quantum Dots in solid matrices in 1984. In Bell Laboratories Louis Brus had two promising post-doctoral researchers, Mounqi Bawendi and Paul Alivisatos, who have become important figures in the field of Quantum Dots. Mounqi Bawendi had later be in charge of a team at MIT (Massachusetts). Paul Alivisatos lead a team at UC Berkeley. In 1993, Mounqi Bawendi was at the origin of the production of the first “high quality” Quantum Dots that have less than 5% size variation in the colloidal suspension. This enabled researchers to control the size of

Quantum Dots and fine-tune the color of their fluorescence. Meanwhile, Philippe Guyot-Sionnest, a young professor at the University of Chicago, was interested in the multiphoton properties of these materials and in 1996, his team synthesized the first Quantum Dots with the core surrounded by a shell. This made it possible to stabilize the properties of the synthesized particles, and to provide easier interaction with their surface chemistry. The first rod-shaped quantum dots were discovered in 2000. At the end of 2000s the teams from MIT, the University of Berkeley, the University of Chicago and Hamburg are particularly active in the field of research on quantum dots. In 2007, the team of Benoit Dubertret produced for the first time Quantum Plates at ESPCI (School of Physics and Chemistry of the City of Paris). This was an extremely important step forward. Compared to conventional Quantum Dots, Quantum Plates are brighter, easier to implement for industrial applications, more heat resistant once encapsulated, and more stable over time. In addition, their emission is naturally polarized and directional. In 2014 a conference to celebrate 30th anniversary on the discovery of Quantum dots was held at ESPCI[2]. A large scale studies are still ongoing in the field of quantum dots.

A very important optical feature of quantum dots (colloidal) is their colour. Each dot emits a different colour depending on its size. When the quantum dots are illuminated by UV light, an electron in the quantum dot can be excited to a state of higher energy. In the case of a semiconducting quantum dot, this process corresponds to the transition of an electron from the valence band to the conductance band[3]. The colour of that light depends on the energy difference between the conductance band and the valence band. If semiconductor particles are made small enough, quantum effects

are exhibited by them. As energy is related to wavelength the optical properties of the particle can be finely tuned depending on its size. Thus, particles can be made to emit or absorb specific wavelengths of light, merely by controlling their size. Light absorption generally leads to an electron being excited from the valence to the conduction band, leaving behind a hole. The electron and the hole can bind to each other to form an exciton. When this exciton recombines (i.e. the electron resumes its ground state), the exciton's energy can be emitted as light. This is called fluorescence. The energy of the emitted photon can be understood as the sum of the band gap energy between the highest occupied level and the lowest unoccupied energy level, the confinement energies of the hole and the excited electron, and the bound energy of the exciton (the electron-hole pair) [4].

The basic rationale for using QDs arises from their unique and fascinating optical properties that are not generally available for individual molecules or bulk semiconductor solids. Quantum dots have proven themselves as powerful fluorescent probes, especially for long-term, multiplexed, and quantitative imaging and detection. Newly engineered quantum dots with integrated targeting, imaging and therapeutic functionalities have become excellent material to study drug delivery in cells and small animals. In comparison with conventional organic dyes and fluorescent proteins, QDs have distinctive characteristics such as size-tunable light emission, improved signal brightness, resistance against photobleaching and simultaneous excitation of multiple fluorescence colors. Recent advances in nanoparticle surface chemistry have led to the development of polymer-encapsulated probes that are highly fluorescent and stable under complex

biological conditions. The new generation of water-soluble QDs solved the problems of quantum yield decrease, chemical sensitivity and short shelf-life previously encountered by the ligand exchange based QD solubilization method. As a result, these particles, linked with bio affinity molecules, have raised new opportunities for ultrasensitive and multicolor imaging of molecular targets in living cells and animal models [5].

## **1.2 CLASSIFICATION OF QUANTUM DOTS**

According to the elemental composition, Quantum dots are widely classified as;

1. II-VI Quantum dots(e.g; ZnTe, ZnSe, ZnS, ZnO,CdS, CdSe,CdTe, HgTe, HgSe, HgS)
2. III-V Quantum dots(e.g; AlSb, AlAs, AlP, GaSb, GaAs, InGaAs, InAs, InP, InN)
3. IV- VI Quantum dots(e.g; PbS, PbSe, PbTe)
4. Silicon Quantum dots
5. Graphene Quantum dots
6. Carbon Quantum dots

An elemental composition expresses which and how many atoms constitute a particular chemical compound. In case of quantum dots, they are classified on the basis of which all elements from different group of the periodic table form the compound. For II-VI quantum dots, elements from group 2 and group 16 form the QD. Among different types of QDs, ZnO,



CdTe, CdSe/ZnS, ZnO etc. with have been used in drug delivery applications, while some of them including CdTe, Cu<sup>+</sup>-doped CdS, CdTe/CdSe, CdSe/CdS, CdS/ZnS, CdSe/ZnS, CdTe/ZnTe, CdTe/CdSe/ZnSe, CdTeSe/CdZnS, and Gd-doped ZnO are found to be beneficial in biological imaging applications (e.g., human hepatic, ovarian, gastric, oral epidermoid, breast, cervix, lung, and pancreatic carcinomas). Several types of QDs, such as CdSeS, CdTe/ZnTe, CdTe, InP/ZnS, CdSe/ZnS, CdSe, and CdS are currently available commercially[6]. Nanocrystals of group II-VI semiconductors, known as quantum dots (QDs), in which electrons and holes are three dimensionally confined within the exciton Bohr radius of the material, are characterized by the exceptional optical properties, such as broad absorption and sharp emission bands as well as size-tunable. III-V quantum dots therefore make nearly ideal single photon sources [7]. Graphene, which basically is an unrolled, planar form of a carbon nanotube therefore, has become an extremely interesting candidate material for nanoscale electronics. Graphene remains highly stable and conductive even when it is cut into devices one nanometer wide. They also show great potential in the fields of photoelectronics, photovoltaics, biosensing, and bioimaging etc. Although developed only recently, inorganic halide perovskite quantum dot systems have exhibited comparable and even better performances than traditional QDs in many fields. By preparing highly emissive inorganic perovskite quantum dots (IPQDs) their superior optical merits could lead to promising applications in lighting and displays. Graphene quantum dots(GQDs) are graphene fragments that are small enough to cause exciton confinement and a quantum size effect. Typically, GQDs have diameters below 20 nm. Carbon quantum dots (CQDs/CDs/C-dots) are another newly emerging quantum

dots, mainly including carbon nanoparticles of less than 10 nm in size. CDs usually exhibit fascinating optical and electro-optical properties due to the quantum confinement and edge effects. Accordingly, CDs are proposed to be promising alternatives for conventional semiconductor-based quantum dots (QDs)[8].

### **1.3 CARBON QUANTUM DOTS**

CDs are assumed to be zero dimensional(0D). They are carbon-based particles with a size range of less than 20 nm with high fluorescence properties. These particles are generally nanocrystallites or amorphous nanostructures. In 2004, carbon nanoparticles with fluorescence were first reported, which were accidentally obtained from the purification of single-walled CNTs[9]. Compared to traditional semiconductor quantum dots and organic dyes, photoluminescent carbon-based quantum dots are superior in terms of high solubility, robust chemical inertness, facile modification and high resistance to photobleaching. They have found wide use in more and more fields during the last few years especially in their synthetic methods, size control, modification strategies, photoelectric properties, luminescent mechanism, and applications in biomedicine, optronics, catalysis and sensor application etc[10]. They have numerous electrochemical and optical properties, which make them ideal candidates for health care applications, particularly in biosensing, bioimaging, drug/gene delivery, and photodynamic/photothermal therapy[11].

## **1.4 PROPERTIES OF CARBON DOT**

CDs are currently being engaged in the area of electrochemistry and electrocatalysis, by virtue of the following advantages; When compared to the other carbon-based nanomaterials, CDs exhibit exceptional charge transferability, enhanced electroconductivity, larger effective surface area, and lesser toxicity, as well as being comparatively cost-effective. The surface of CDs possesses abundant functional groups such as hydroxyl, carboxyl, amine, etc., which can deliver a large number of sites for the surface modification, as well as for the enhanced electrocatalytic activity by accelerating the intermolecular electroconductivity. CDs can remarkably enhance electrocatalysis process during the electrochemical reactions such as oxygen evolution reaction (OER), hydrogen evolution reaction (HER), oxygen reduction reaction (ORR), and alcohol oxidation reaction (AOR). The above-mentioned merits of CDs make them ideal electrocatalytic agents to serve desired electrochemical applications. CDs display superior electrical conductivity, and when they are employed as electrocatalysts during the electrocatalytic reactions, the Schottky barrier occurring at an electrolyte catalyst junction can be readily removed, which can thereby confirm the effective energy transformation. Moreover, owing to the excellent electrical conductivity, CDs can very rapidly transfer electrons during electrochemical reactions. During electrochemical reactions, CDs can efficiently act as the active centers by virtue of their excellent electroconductivity, numerous defect sites and active edges, as well as their large surface area-to-volume ratio. Henceforth, when CDs are fused together with conductive materials, they can dramatically facilitate the electrochemical performance and characteristics[12]. When CDs are doped

using heteroatoms such as nitrogen, phosphorous, sulfur, boron, etc., their electronic attributes can be significantly improved due to the intramolecular charge transferability. Electronic structural arrangement, when CDs are doped by heteroatoms such as nitrogen, phosphorous, sulfur, boron, etc., results in the desired change in their chemical structure, whereas the electric charge can be efficiently transferred from the adjacent carbon atoms. The heteroatom-doped CDs show exceptional electrochemical performance due to the enhancement of intrinsic activity of surface functional sites, the distortion of their electronic configuration, tuning of local densities, as well as the acceleration of adsorption and desorption phenomenon[13].

Due to the presence of large numbers of active functional groups on the surfaces of CDs, as well as their long-term chemical stability in a wide range of solvents, they are proved to be the ideal nanomaterials in terms of improving the chemical stability of hybrid catalysts [14]. Furthermore, CDs can be used as the supporting materials during the preparation of their hybrid nanocomposites with metals and metal oxides, which can lead to the prevention of agglomeration and thereby, increase in the electrocatalytic activity. In addition, CDs can demonstrate good stability in aqueous media due to the electrostatic stabilization, which can facilitate the steadiness of hybrid catalysts. Due to the  $\pi$ - $\pi^*$  transition of C=C bonds in the structure of CDs, their absorbance is generated in the short-wavelength region. CDs reveal intense optical absorbance from 260 to 320 nm (i.e., in the UV region). Their absorbance range may vary depending on the type of CD, due to the surface functional groups, as well as their surface passivation[15]. By virtue of the astonishing optical features offered by fluorescent CDs, they have been severely used in diverse health care applications, especially

in the field of biosensing, bioimaging, and therapy development. It is of great importance to study and understand the optical properties of CDs in order to prepare a variety of CDs for serving bio-applications.

Fluorescence is the emission of light by a substance that has absorbed light or other electromagnetic radiation. It is a form of luminescence. In most cases, the emitted light has a longer wavelength, and therefore a lower photon energy, than the absorbed radiation. A perceptible example of fluorescence occurs when the absorbed radiation is in the ultraviolet region of the spectrum (invisible to the human eye), while the emitted light is in the visible region; this gives the fluorescent substance a distinct color that can only be seen when exposed to UV light. Fluorescent materials cease to glow nearly immediately when the radiation source stops, unlike phosphorescent materials, which continue to emit light for some time after. CDs exhibit fluorescence property.

Up-conversion fluorescence: It is the phenomenon, where the excitation wavelength is larger than the emission wavelength. The up-conversion fluorescence property can be observed in the CDs that are synthesized through ultrasonic treatment. Larger excitation wavelength results in the reduction of background auto fluorescence, which is significant for the bioimaging application.

Down-conversion fluorescence: The luminescent mechanism of CDs is yet to be deeply investigated. However, several origins responsible for the fluorescence of CDs usually include multi-emissive centers, free zigzag sites, self-trapped excitons, quantum confinement effects, special edge

defects, their conjugated structures, and surface states. Since CDs are 0D quantum confined nanomaterials, their fluorescence can be accredited to the presence of an electron-hole pair in their system. As the size of CDs increases, their energy gap decreases. Therefore, the fluorescence property of CDs can be regulated by altering their quantum confinement effect. The surface state phenomena due to the existence of surface functional groups and surface oxidation, is one of the other mechanisms for the origin of CDs fluorescence[15]. The surface oxidation incurred by oxygen-containing groups at the edge of CDs, is responsible for creating the surface defects that results in the fluorescence.

**Emission properties:** Different fluorescence emissions of CDs can be obtained by controlling their excitation wavelength, which can be achieved by regulating several physicochemical parameters during CDs' synthesis. For instance, the fluorescence of CDs is highly influenced by pH, concentration, as well as temperature. The pH dependent emission is because of the functional group protonation and deprotonation on their surfaces; the concentration-dependent fluorescence is due to the surface state emission; whereas the temperature-dependent emission is the result of non radiative decay occurring at the surface of CDs.

**Chemical stability and photobleaching properties:** Fluorescence bioimaging or biosensing requires long emission lifetimes and stable fluorescence signal. This can be achieved with the help of CDs, since they have the tendency to produce stable signals when stored in an aqueous environment . Furthermore, CDs can emit strong fluorescence for long time (i.e., up to a

year). Generally, CDs are resistant to a broad pH range (i.e., from 3 to 12), therefore they demonstrate excellent impedance for photobleaching[16].

The room-temperature phosphorescence (RTP) property of CDs is of great importance due to its long lifetime. Two aspects should be ideally taken into a consideration for obtaining RTP. The first involves the suppression of non-radiative transitions by restricting rotation and vibration, while the second one aims to facilitate the inter system crossing ability by enriching the spin-orbit coupling through the use of transition metals. Alternatively, RTP can also be achieved by employing CDs with enormously cross-linked structures containing non-conjugated groups. The production of RTP in aqueous media is relatively challenging, since phosphorescence quenching is commonly observed in water because of the solvent-assisted relaxation, as well as due to the existence of dissolved oxygen[17].

In chemiluminescence (CL), the light is produced via a chemical reaction. Under appropriate conditions in redox reaction, CDs can generate CL in aqueous solvents, where the unstable products are produced from intermediate radicals during CL. CDs can generate CL either due to their excitation after direct oxidation or through the enhancement or inhibition of their luminescence. CDs are able to emit photons in the visible region under electrical excitation, which is important to study their electrochemiluminescence (ECL) property. Owing to the enhanced electron transfer due to a large amount of  $sp^2$  carbon in CDs, it results in a stable compound[18]. The outstanding electronic properties of carbon-based quantum dots as electron donors and acceptors, causing chemiluminescence

and electrochemical luminescence, endow them with wide potentials in optronics, catalysis and sensors application[19].

## **1.5 APPLICATIONS OF CARBON DOT**

One of the most fascinating features of CDs, both from fundamental and application-oriented perspectives, is their PL. Since their discovery carbon quantum dots and their structurally related cousins graphene quantum dots have attracted significant and growing interest in both scientific and technology circles. This interest, also reflected by the almost exponential growth of scientific articles published on the subject, stems primarily from the unique physical properties of Carbon-Dots, particularly their luminescent properties. CDs, similar to inorganic fluorescent semiconductor nanoparticles exhibit tunable fluorescence emission, in other words they emit light in different colors. This useful property has naturally been a major driving force in the significant expansion of Carbon-Dot research. Due to their higher photostability, good water solubility, environmentally friendly nature, the ease of synthesis methods combining the strong fluorescence and optical properties make CDs promising materials with great potential compared to semiconductor quantum dots and toxic organic dyes in the wide range of application fields. Especially, CDs are considered as safe with no vital toxicity on the various cell lines for in vitro applications and have shown excellent biocompatibility for in vivo biomedical applications, including cell imaging, cancer therapy, drug/gene carrier vehicles, diagnosis of diseases, etc[20].



Several studies have reported that CDs exhibit PL emission in the near-infrared spectral region under the NIR irradiation that can be an advantage for chemo-photothermal (PTT) and photodynamic (PDT) treatment for different tumors. Cationic CDs have shown great potential as gene carriers and delivery applications because of their ability of electrostatic interaction with positively charged functionalized CDs and negatively charged nucleic acids. Fluorescence CDs can be used as sensors for the detection and identification of a wide range of analytes, that is, cations, anions, drugs, small molecules, and macromolecules, depending on high sensitivity and selectivity, and the easy operation as benign biocompatible, and low-cost device applications [21]. More recently, CDs have been used in energy conversion and storage as well as electrocatalytic and photocatalytic devices, owing to their outstanding features such as low cost, broad optical absorbance, high photo and chemical stability, environmental friendless and nontoxicity, and scalable synthesis methods.

The unique photoluminescence (PL) properties of CD including tunable emission, nonblinking, and excellent photostability enable them great potential in wide applications ranging from photoelectric device, fluorescence sensing, to bioimaging and nanomedicines. Moreover, one of their most intriguing property is their pH-dependent PL. As the pH changes, the PL spectra or intensity of C-dots would change accordingly. It is well-known that pH plays key role in industrial, agricultural, environmental, and biomedical field[22]. It is of great significance for both scientific research and real-word applications to monitoring pH in disease diagnosis, environmental examination, food and beverage analysis, and so on. pH-sensitive nanoprobess based on organic dyes and nanocarriers have been

developed to overcome the limitations of photobleaching, phototoxicity, and interference from background auto fluorescence of traditional organic fluorescent dye. However, it is still difficult to achieve long-term and biological damage-free pH monitoring due to the poor biocompatibility and large particle size of organic dyes and nanocarriers. C-dots with small size, excellent photostability, and good biocompatibility have the potential to provide solutions for pH sensing in environmental, pharmaceutical, and especially in vivo medical applications. In recent years, many synthetic methods have been developed to prepare pH-sensitive CD. Interestingly, although the synthesis methods, raw materials, structure, and morphology of CDs are quite different, most CDs possess pH-sensitive PL properties, despite their pH response behaviors are different. The typical understanding of the mechanism of pH-sensitive PL mainly focused on the deprotonation and protonation of acidic and basic groups in ground or excited states, which could change the property and the rate of transition processes, and finally affect the PL spectrum and intensity of the fluorophores. There are also many researchers who believed that the pH sensitivity of C-dots was caused by the pH induced aggregation of CD. Surface modification is a useful approach to expand the analytical application and target detection of carbon dots. The produced probes can incorporate with non-radiative fluorescence quenching strategies for target recognition. Common approaches, including inner filter effect (IFE), fluorescence resonance energy transfer (FRET), and photoinduced electron transfer (PET), are all compatible with this material. For instance, carbon dots can be modified with organic dyes to detect hydrogen sulfide (H<sub>2</sub>S) via dye reduction induced FRET effect. In addition, ethylenediamine modified CD can detect silver nanoparticles via particle aggregation induced IFE phenomenon[23].

CDs can often display high optical absorptivity across a wide visible light range making them a possible alternate sensitizer in DSSCs. The current most advanced DSSCs typically employ Ruthenium-based sensitizers. The dilemma lies in that Ru-based sensitizers generally offer superior performance but they are often time-consuming to synthesize and rely on the Ruthenium-metal center, which is scarce and expensive, urgently necessitating a sustainable, environmentally friendly substitute. When CDs are used as a sensitizer, photo-charged surface recombination is also observed, which may be the cause of low current density. The study on the use of CD as a sensitizer in the DSSC device also reached a similar conclusion that the CD helps to assist the charge separation and increase the concentration of charge carriers available in the photoreactions. The difference in CD and gaps allows the transfer of photo-generated electrons from CDs to ZnO. Efficient charge separation and electron transfer to the electrode surface result in higher performance of CD solar cells, which may benefit from the good anchoring of CDs on ZnO nanoparticles and the appropriate work function[24].

## **1.6 SYNTHESIS OF CARBON DOT**

In recent years, great progress has been made in the preparation of CDs. Depending on the carbon source used, the synthesis methods of CDs can generally be divided into top-down and bottom-up approaches . The top-down method is mostly used in the early stage of research and usually prepares CDs by stripping and cutting large-size carbon materials with physical or chemical ways; and the bottom-up method aggregates small

organic molecule into CDs by means of chemistry. These two approaches can meet the different requirements of small particle size and excellent optical properties of CDs to some extent.

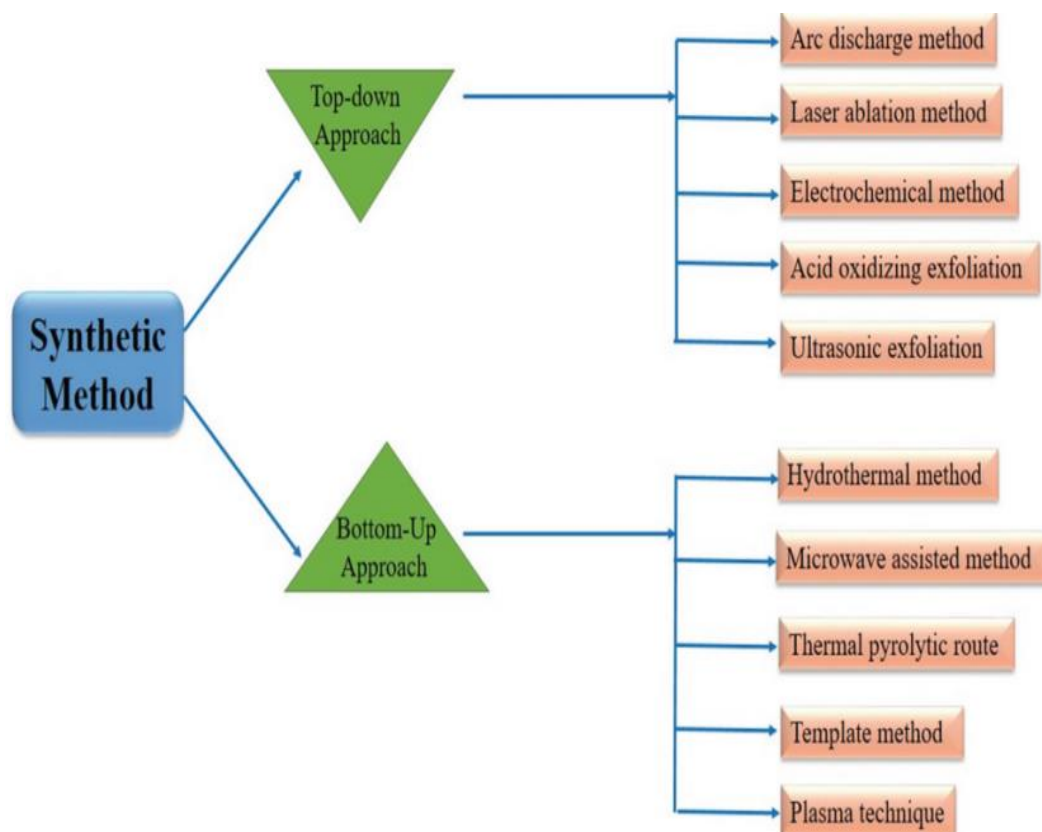


Fig 1.1: Different synthetic methods of CD.

### 1.6.1 Top-Down Approach

In the top-down approach, physical or chemical processes are often applied to strip and cut large-sized carbon materials to obtain small-sized CDs, which are more common in the early stages of CDs research. At present, carbon-based materials with large particle size such as graphite, carbon

nanotubes and activated carbon have been used for the preparation of nanosized CDs. And the treatment method has also been extended to arc, laser, chemical reagent or high potential methods. However, this kind of methods are usually carried out under the conditions of high acidity, high potential and high energy, which are relatively difficult to control. Consequently, there are scarce reports in the synthesis of CDs in recent years. Mechanical milling, nanolithography, laser ablation, sputtering and thermal decomposition are some of the most widely used synthesis methods.

**Mechanical milling:** Among the various top-down methods, mechanical milling is the most extensively used to produce various nanoparticles. The mechanical milling is used for milling and post annealing of nanoparticles during synthesis where different elements are milled in an inert atmosphere. The influencing factors in mechanical milling is plastic deformation that leads to particle shape, fracture leads to decrease in particle size and cold-welding leads to increase in particle size .

**Nanolithography:** Nanolithography is the study of fabricating nanometric scale structures with a minimum of one dimension in the size range of 1 to 100 nm. There are various nanolithographic processes for instance optical, electron-beam, multiphoton, nanoimprint and scanning probe lithograph. Generally lithography is the process of printing a required shape or structure on a light sensitive material that selectively removes a portion of material to create the desired shape and structure. The main advantages of nanolithography is to produce from a single nanoparticle to a cluster with

desired shape and size. The disadvantages are the requirement of complex equipment and the cost associated.

**Laser ablation:** Laser Ablation Synthesis in Solution (LASIS) is a common method for nanoparticle production from various solvents. The irradiation of a metal submerged in a liquid solution by a laser beam condenses a plasma plume that produces nanoparticles. It is a reliable top-down method that provides an alternative solution to conventional chemical reduction of metals to synthesis metal-based nanoparticles. As LASIS provides a stable synthesis of nanoparticles in organic solvents and water that does not require any stabilizing agent or chemicals it is a ‘green’ process.

**Sputtering:** Sputtering is the deposition of nanoparticles on a surface by ejecting particles from it by colliding with ions. Sputtering is usually a deposition of thin layer of nanoparticles followed by annealing. The thickness of the layer, temperature and duration of annealing, substrate type, etc. determines the shape and size of the nanoparticles.

**Thermal decomposition:** Thermal decomposition is an endothermic chemical decomposition produced by heat that breaks the chemical bonds in the compound [30]. The specific temperature at which an element chemically decomposes is the decomposition temperature. The nanoparticles are produced by decomposing the metal at specific temperatures undergoing a chemical reaction producing secondary products[30].

### **1.6.2 Bottom-Up Approach**

Bottom-up, or self-assembly, approaches use chemical or physical forces operating at the nanoscale to assemble basic units into larger structures. As component size decreases in nanofabrication, bottom-up approaches provide an increasingly important complement to top-down techniques. Inspiration for bottom-up approaches comes from biological systems, where nature has harnessed chemical forces to create essentially all the structures needed by life. A number of bottom-up approaches have been developed for producing nanoparticles, ranging from condensation of atomic vapours on surfaces to coalescence of atoms in liquids[31]. In the bottom-up approach, the energy of microwave, hydrothermal and ultrasound is usually applied to aggregate small organic molecules or oligomer precursors to synthesize nanometer-sized CDs. Under the environment of high radiation, high heat and high frequency, the generated CDs can be equipped with both high QY and excellent optical properties. This kind of method has been favored by researchers in the preparation of CDs in recent years, because the preparation and operation are simple, reaction conditions are controllable and raw materials are inexpensive.

**Sol-gel:** The sol – a colloidal solution of solids suspended in a liquid phase. The gel – a solid macromolecule submerged in a solvent. Sol-gel is the most preferred bottom-up method due to its simplicity and as most of the nanoparticles can be synthesised from this method. It is a wet-chemical process containing a chemical solution acting as a precursor for an integrated system of discrete particles. Metal oxides and chlorides are the typically used precursors in sol-gel process. The precursor is then dispersed

in a host liquid either by shaking, stirring or sonication and the resultant system contains a liquid and a solid phase. A phase separation is carried out to recover the nanoparticles by various methods such as sedimentation, filtration and centrifugation and the moisture is further removed by drying .

**Spinning:** The synthesis of nanoparticles by spinning is carried out by a spinning disc reactor (SDR). It contains a rotating disc inside a chamber/reactor where the physical parameters such as temperature can be controlled. The reactor is generally filled with nitrogen or other inert gases to remove oxygen inside and avoid chemical reactions. The disc is rotated at different speed where the liquid i.e. precursor and water is pumped in. The spinning causes the atoms or molecules to fuse together and is precipitated, collected and dried. The various operating parameters such as the liquid flow rate, disc rotation speed, liquid/precursor ratio, location of feed, disc surface, etc. determines the characteristics nanoparticles synthesised from SDR.

**Chemical Vapour Deposition (CVD):** Chemical vapour deposition is the deposition of a thin film of gaseous reactants onto a substrate. The deposition is carried out in a reaction chamber at ambient temperature by combining gas molecules. A chemical reaction occurs when a heated substrate comes in contact with the combined gas [32]. This reaction produces a thin film of product on the substrate surface that is recovered and used. Substrate temperature is the influencing factor in CVD. The advantages of CVD are highly pure, uniform, hard and strong nanoparticles. The disadvantages of CVD are the requirement of special equipment and the gaseous by-products are highly toxic [33].



**Pyrolysis:** Pyrolysis is the most commonly used process in industries for large scale production of nanoparticle. It involves burning a precursor with flame. The precursor is either liquid or vapour that is fed into the furnace at high pressure through a small hole where it burn . The combustion or by-product gases is then air classified to recover the nanoparticles. The advantages of pyrolysis are simple, efficient, cost effective and continuous process with high yield.

**Biosynthesis:** Biosynthesis is a green and environmental friendly approach for the synthesis of nanoparticles that are nontoxic and biodegradable. Biosynthesis uses bacteria, plant extracts, fungi, etc. along with the precursors to produce nanoparticle instead of convention chemicals for bioreduction and capping purposes. The biosynthesised nanoparticles has unique and enhanced properties that finds its way in biomedical applications [25].

**Hydrothermal:** This process can be defined as an heterogeneous reaction in the presence of aqueous solvents or mineralizers under high pressure and temperature conditions to dissolve and recrystallize materials that are relatively insoluble under ordinary conditions. Hydrothermal has been defined as any heterogeneous chemical reaction in the presence of a solvent (whether aqueous or non-aqueous) above the room temperature in a closed system [26]. Material processing under hydrothermal conditions requires a pressure vessel capable of containing a highly corrosive solvent at high temperature and pressure. An ideal hydrothermal apparatus popularly known as an autoclave, or reactor, or pressure vessel. However, an ideal

hydrothermal autoclave should be Inert to acids, bases and oxidizing agents, Ease of assembly and disassembly, Sufficient length to obtain desired temperature gradient, Leak-proof with unlimited capabilities to the required temperature and pressure range, Rugged enough to bear high pressure and temperature experiments for long periods with no damage so that no machining or treatment is needed after each experimental run[27].



Fig 1.2 : Autoclave reactor

Among various technologies available today in advanced materials processing, the hydrothermal technique occupies a unique place owing to its advantages over conventional technologies. It covers processes like hydrothermal synthesis, hydrothermal crystal growth leading to the preparation of fine to ultra fine crystals, bulk single crystals, hydrothermal transformation, hydrothermal sintering, hydrothermal decomposition, hydrothermal stabilization of structures, hydrothermal dehydration, hydrothermal extraction, hydrothermal treatment, hydrothermal phase equilibria, hydrothermal electrochemical reactions, hydrothermal recycling,

hydrothermal microwave supported reactions, hydrothermal mechanochemical, hydrothermal sonochemical, hydrothermal electrochemical processes, hot pressing, hydrothermal metal reduction, hydrothermal corrosion, and so on. The hydrothermal processing of advanced materials has lots of advantages and can be used to give high product purity and homogeneity, crystal symmetry, metastable compounds with unique properties, narrow particle size distributions, a lower sintering temperature, a wide range of chemical compositions, single-step processes, dense sintered powders, sub-micron to nanoparticles with a narrow size distribution using simple equipment, lower energy requirements, fast reaction times, lowest residence time, as well as for the growth of crystals with polymorphic modifications, the growth of crystals with low to ultra low solubility, and a host of other applications[28]. Also, the duration of experiments is being reduced at least by 3-4 orders of magnitude, which will in turn, make the technique more economic. Besides, for processing nanomaterials, the hydrothermal technique offers special advantages because of the highly controlled diffusivity in a strong solvent media in a closed system. Nanomaterials require control over their physico-chemical characteristics, if they are to be used as functional materials. As the size is reduced to the nanometer range, the materials exhibit peculiar and interesting mechanical and physical properties: increased mechanical strength, enhanced diffusivity, higher specific heat and electrical resistivity compared to their conventional coarse-grained counter-parts due to a quantization effect [29].

The hydrothermal method has many advantages such as highly homogeneous crystalline product can be obtained directly at a relatively

lower reaction temperature, it favours a decrease in agglomeration between particles, narrow particles size distribution, phase homogeneity, and controlled particle morphology; it also offers a uniform composition, purity of the product, monodispersed particles, control over the shape and size of the particles, and so on [30]. The hydrothermal technique is highly promising for reactions involving volatiles, as they attain the supercritical fluid state and supercritical fluids are known for their greater ability to dissolve non-volatile solids. Further, the technique facilitates issues like energy saving, the use of larger volume equipment, better nucleation control, avoidance of pollution, higher dispersion, higher rates of reaction, better shape control, and lower temperature operations in the presence of the solvent. Although the hydrothermal technique offers some special advantages for processing advanced materials, there are some disadvantages. The Processes are difficult to control and there are some Limitation of reliability and reproducibility [31].

## **1.7 SOURCES OF CARBON DOT**

The synthesis of carbon dots (CDs) from green precursors has received considerable attention recently. Till now, various synthetic strategies, e.g. hydrothermal method, solvothermal method, microwave method, ultrasonic method, plasma method, laser ablation and diverse precursors have been developed to prepare CDs. In particular, low-cost, widespread, and eco-friendly raw biomass resources hold great potentials as precursors to generate CDs. In this respect, various biomass precursors, such as hair, grass, leaves, fruits, eggs, and olive have been explored to produce CDs[32]. Carbon sources in the form of natural materials that are

abundant in nature such as plants. Many researchers have used parts of plants as a carbon source. The plant's part is in the form of bulbs, flowers, leaves and fruit. Bulbs are one part of the plant that lies in the soil, or more precisely the roots of plants. Researchers use these bulbs as a natural carbon source via hydrothermal treatment such as rose-heart radish, carrots, and sweet potato[33]. Carrot can be used as a carbon source for the fluorescent CDs by hydrothermal treatment. Carrot roots is one of the important plants which contain carbohydrates, carotenoids, polyphenols, and dietary fibres [34]. Similarly CDs can be prepared from garlic, onion, ginger, water chestnut etc[35]. Several studies have been carried out using flowers as well as bulbs as a source of carbon such as *Syringa obtata Lindl*, *Magnolia liliiflora* and *Abelmoschus manihot*. Leaves are generally a green color, grow from twigs and have a function as a catcher energy from the sunlight for photosynthesis. It was reported that bamboo leaves can be used as a carbon source via green hydrothermal method for high quantum yield carbon quantum dots[36]. Also reported green synthesis of CDs via hydrothermal treatment using coriander leaves and successfully shows UV light with bright green luminescence. The diameter of CDs about 4.158 nm and the quantum yield is 6.48% [37]. Similar results were reported by researchers which successfully used tea plants such as oolong tea [38] and waste tea [39] as a CDs source. Various fruits can also be used as a carbon source for the preparation of CDs. Fruits such as watermelon, strawberry, orange and dragon fruit, apple and banana[40]. Many other fruits, vegetables, juices, human derivatives, beverages, and bakery products, food waste uses as green sources. In this work we have focused on crustacean wastes as the source of carbon dot.



Fig 1.3: Different sources of carbon dot

### 1.7.1 CRUSTACEAN WASTE: AS A SOURCE OF CARBON DOT

Marine crustacean wastes such as squilla, krill, prawns, crab and lobster shells are industrial by-products. The worldwide seafood industries are estimated to generate tons of crustacean waste in one year. The discarding of such large quantity of crustacean waste is a serious environmental problem especially because of they are resist to bio degradation, insoluble in water and to process the waste is a high cost. The crustacean waste contains a large quantity of chitin and small quantity of proteins, minerals (mainly calcium), lipids and pigments. Chitin and its derivatives have great economical value because of their numerous applications in food, cosmetics, pharmaceuticals, textile industries, waste water treatment and

agriculture. Several techniques to extract chitin from different sources have been reported [41]. However, the traditional chitin extraction processes employ harsh chemicals at elevated temperatures for a prolonged time which can harm its physico chemical properties and are also held responsible for the deterioration of environmental health. In view of this, green extraction methods are increasingly gaining popularity due to their environmentally friendly nature. The bio extraction of chitin from crustacean shell wastes has been increasingly researched at the laboratory scale. However, the bio extraction of chitin is not currently exploited to its maximum potential on the commercial level. Crustacean shell is composed of 30–40% proteins, 30–50% mineral salts, and 13–42% of chitin occurring in  $\alpha$ -,  $\beta$ -, and  $\gamma$ -forms. In the processing of shrimps for human consumption, between 40 and 50% of the total mass is waste and 40% of this waste is chitin. A small part of the waste is usually dried and utilized as chicken feed, while the rest is dumped into the sea, which is one of the main pollutants in coastal areas. The utilization of shellfish waste has thus been able to solve environmental problems, being an alternative waste disposal method [42]. Chitin extraction involves alkaline extraction of organics and acid solubilization/decomposition of minerals, subsequent to protein removal. During such extractions, the chitin molecule also suffers some structural changes, including a moderate degree of deacetylation. Chitosan, is obtained on substantial deacetylation through alkaline treatment of chitin under severe conditions. The use of cost-free seafood waste such as prawns shell as new carbon source for the green synthesis of fluorescent C-dots is an innovative method. This method can recycle the environmental wastes for the preparation of CD. Further more these CDs exhibits pH sensing application [43].

## 1.8 ANTIBACTERIAL ACTIVITY OF CARBON DOT

Bacteria and fungus exist in every corner of the world, and their infection is one of the biggest global challenges to human health [44]. Notably, the overuse or abuse of antibiotics in the long term lead to the emergence of multiple drug-resistant (MDR) bacteria, which increases the difficulty of infectious diseases therapy. Also, fungus and bacteria can cause widespread plant diseases. Pesticides are used widely for the resistance of plant diseases, while their continuously over-use always leads to severe environmental problems [45]. Up to now, great efforts have been paid in the development of antibiotics, drugs and antimicrobial materials. In recent years, the carbon dots have gradually become a rising star in the nanocarbon family, due to their benign, abundant and inexpensive nature. CDs show a strong broad-spectrum antibacterial activity and antifungal activity, efficiently inhibiting the growth of *S.aureus*, *E.coli* and many others. The bacteriostatic or bactericidal effect of CDs can be exerted through several major routes, including physical and mechanical damage to the bacterial membrane, destruction of bacterial cell wall with consequent leakage of cytoplasmic material, inactivation via Laser irradiation-assisted photothermal therapy (PTT) effects due to localized temperature increase [46]. Bacterial inactivation promoted by membrane damage is also a commonly observed consequence of CD intercalation in the bacterial membrane etc [47].

With industrial development, antibacterial material has become an extremely urgent problem. Bacterial infection has caused many harmful events. In order to solve this problem, many methods and reagents have



been used, among which semiconductor photocatalyst is an ideal choice. Particularly, ZnO has attracted much attention for its excellent antibacterial activity and biocompatibility. Massive research works showed that ZnO can produce a variety of active free radicals with strong oxidizing properties under light conditions, which can decompose the organic pollutants and bacteria quickly [48]. However, the response range to visible light of ZnO nanoparticles is narrow and the photogenerated electrons and holes are prone to recombination easily, which have restricted the application of pure ZnO in actual application extremely. CDs are regarded as the potential choice of photocatalyst due to its coordinated fluorescence emission in visible and near infrared regions. CDs can be used to modify the semiconductor surface by irradiation in the visible light region and have stronger photocatalytic activity. Researches have proved that modify semiconductor with CDs can improve its photocatalytic activity when irradiated with visible light. Moreover, the CDs attracted more attention than other carbon based materials for their higher photo-induced electron transfer and up-conversion properties. Many researchers have synthesized CD-TiO<sub>2</sub> nanocomposites to improve its photocatalytic activity respectively. This strategy was also suitable for improving the photocatalytic activity of ZnO semiconductor. Other researchers have synthesized CD-ZnO nanocomposites to investigate its photocatalytic property, while the antibacterial activity of CD-ZnO nanocomposite has not been noticed.

Later on many studies were conducted in order to study the enhancement of antibacterial activity of CD-ZnO nanocomposite. The research about the antibacterial activity of CDs decorate Copper doped ZnO nanocomposite (

CD-ZnO-Cu) have not been reported to the best of our knowledge. In the present work, we have prepared the CD-ZnO nanocomposite and CD-ZnO-Cu nanocomposite, and their visible light-activated antibacterial activities were also studied [49].

## **1.9. LITERATURE STUDY**

Many studies have been conducted to study versatile characteristics of the C-dots, their application and preparation methods.

A. L. Himaja et al (2014) Synthesized Carbon dots (C-dots) from biodegradable kitchen waste which is a much researched subject now-a-days. Nanometer sized carbon particles with unique optical properties were observed during the study. Peels of fresh cucumber/pineapple were taken and washed thoroughly with water. Peels were then crushed into a paste using a home-use mixer grinder and mixed with distilled water. This mixture was then heated and filtered resulting in a yellow colored solution. The solution was then centrifuged to remove any heavier particles present. Then, solution was taken by decantation. The former was a clear pale yellow colored solution. The solution was then refluxed and later allowed to cool down naturally. It was then centrifuged. It was then suspended with 1N NaOH. A clear and bright yellow suspension of C-dots was obtained which showed green fluorescence when checked under UV light. It was then characterized using UV-Visible Spectroscopy. The C-dots obtained from cucumber peel were observed to have two absorption bands at 267 nm and 328 nm. UV-visible absorption peaks occurred at 317 nm and 269 nm for C-dots obtained from pineapple peel. The C-dots obtained from cucumber

peel exhibited a strong characteristic absorption at  $3419.88\text{ cm}^{-1}$  which was due to O-H stretching. Another medium stretch was observed at  $1597.9\text{ cm}^{-1}$  and also at  $1408.87\text{ cm}^{-1}$  which indicated the presence of C-C aromatic rings. A small C-O stretch was also observed at  $1112.49\text{ cm}^{-1}$ . The FTIR spectrum showed that the C-dots obtained from pineapple peel exhibited a strong characteristic absorption at  $3395.14\text{ cm}^{-1}$  which was due to O-H stretching. Another medium stretch was observed at  $1599.38\text{ cm}^{-1}$  and also at  $1407.50\text{ cm}^{-1}$  which indicated the presence of C-C aromatic rings. A small C-O stretch was also observed at  $1053.76\text{ cm}^{-1}$ . All these stretches indicate that the C-dots are highly water soluble in nature. The TEM image also revealed that the particles were completely dispersed in water. The spherical morphology was clearly visible with the size of C-dots being  $\sim 50\text{ nm}$  in diameter. The XRD pattern of C-dots which have an intense peak at  $31.428^\circ$  and  $29.781^\circ$  respectively. These results indicate the crystalline nature of C-dots [50].

Xin feng et al (2015) synthesized N-doped carbon dots successfully via one-step hydrothermal method by using edible winter melon as the source material. Mono-dispersed CDs  $4.5\text{--}5.2\text{ nm}$  in diameter were achieved in a quantum yield of  $7.51\%$ . It was extracted from crushed winter melon. Homogeneous and water-soluble CDs can be directly prepared by a hydrothermal process at  $180^\circ\text{C}$  for  $2\text{ h}$  after subsequent centrifugation and dialysis. The morphology and particle size of CDs were examined by TEM and DLS analysis reveals that the N-doped CDs are uniform and regularly spherical in shape. The obtained N-doped CDs with a narrow size distribution exhibit outstanding aqueous dispersibility, strong photoluminescence, and excellent photostability. Based on the favorable

biocompatibility and low cytotoxicity, the N-doped CDs were internalized into hepG2 cells as cell-imaging agents showing bright blue fluorescence at UV light excitation. XPS and FTIR measurements were performed to identify the effective incorporation of nitrogen and surface functional groups of CDs. From a survey scan of the XPS spectrum, three distinct peaks were observed [51].

Wen Liu et al (2016) reported a simple, green and low cost way to synthesize fluorescent CDs with well defined size using one-pot hydrothermal treatment of rose-heart radish. More over, synthesized CDs generate strong response to  $\text{Fe}^{3+}$  ions and gives rise to the fluorescence quenching. This phenomenon was used to develop a fluorescent method for facile detection of  $\text{Fe}^{3+}$ . CDs were synthesized via a hydrothermal method using roseheart radish as carbon precursor. In a typical synthesis, 2.0 g fresh chopped rose-heart radish was added into 10 mL ultrapure water and stirred for 30 min. The mixture was then transferred into a 25 mL Teflon-lined autoclave and heated at 180 °C for 3 h in an oven. Ultimately, the suspension was subjected to centrifugation (13000 rpm, 15 min) and passed through a 0.22 m micron filter and dialysis against deionized water. The optical properties of CDs were explored using UV–vis absorption spectra. The UV–vis absorption spectra of the N-CDs dispersed in water showed a strong absorption peak at 281.5 nm corresponding to the  $n-\pi^*$  transition of C=O bond . Very bright blue luminescence was seen under the illumination of UV (365 nm) Light in aqueous solution. The PL stability of CDs was investigated. The size distribution and morphology of the obtained N-CDs were characterized by TEM. The surface functional groups and

element states of N-CDs were also characterized by the XPS. The FTIR spectrum shows the characteristic absorption bands at 3416 cm<sup>-1</sup> corresponding to the stretching vibrations of O–H and N–H.<sup>48</sup> The peak at 2926 cm<sup>-1</sup> is ascribed to the C–H bonds. The absorption bands at 1624 cm<sup>-1</sup> and 1404 cm<sup>-1</sup> are due to the C–O stretching vibrations and C–N stretching vibrations, respectively [52].

Gangaraju Gedda et al (2016) proposed a facile, economical and effective green method was for the synthesis of fluorescent carbon dots from prawn shells. In the first step, pure chitin was obtained from prawn shells by the deproteinization with NaOH and followed by the demineralization process with HCl at room temperature. proteins, other organic moieties and minerals were removed in deproteinization and demineralization steps. The resulting chitin was converted to chitosan via deacetylation by the chemical treatment with NaOH. Finally, the obtained chitosan was converted to C-dots by the hydrothermal carbonizations process. The prepared C-dot solution was yellowish in color under normal light and exhibited intense blue luminescence under UV excitation. Photoluminescence (PL) properties of these blue fluorescent C-dots were inspected using UV-Vis spectroscopy and fluorescence spectroscopy. From the UV-Vis spectra, it can be seen that there are two absorption peaks, one at 280 nm (sharpen absorption peak) and another around 330 nm corresponding to  $\pi \rightarrow \pi^*$  and  $n \rightarrow \pi^*$  in carbon dot surface. Fourier transform infrared (FTIR) spectroscopy was employed to investigate the C-dot surface, functional groups. The morphology, size, nature and elemental composition of the prepared C-dots studied using TEM. The TEM images of C-dots reveal that the C-dots are homogeneous, and particles dispersed in a spherical shape. The resulting C-dots diameter

ranges from 2 to 8 nm with an average size of 4 nm. XRD studies and EDXS studies are also conducted. These C-dots used as effective sensing probes for  $\text{Cu}^{2+}$  detection and found that they exhibits excellent selectivity and sensitivity toward  $\text{Cu}^{2+}$  with a low detection limit of 5 nm[53].

Ting-yi wang et al (2017) synthesized Multicolor Functional Carbon Dots via One-Step Refluxing Synthesis. In this study, carbon dots carrying different emission colors are prepared through a one-step refluxing process. The emission of these materials can be well-tuned by sodium hydroxide content in the precursor solution. In this case multicolor carbon dots synthesis is demonstrated With the control of base content in the precursor solution. Carbon dots of three different colors, including blue, green, and yellow, are prepared by the one-step refluxing method. With the use of 0.4, 0.2, and 0.1 M NaOH, blue, green, and yellow carbon dots were produced, respectively. The solutions were cooled down to room temperature and dialyzed for one day. Thereafter, the dialysis-purified solutions were freeze-dried in a lyophilizer for 2 days to collect the carbon dot product powders. These carbon dots were then suspended in the PBS buffer and stored at  $-20^{\circ}\text{C}$  in dark before further use. It was characterized using XRD and EDS. UV-vis and fluorescence spectrum were used to illustrate the unique optical properties of these materials [54].

Later Jue Liang et al (2018) synthesized highly efficient red-emissive carbon dots (CDs) that still impedes widespread applications of CDs in bioimaging. Herein, a facile, isolation-free synthesis of deep red (600–700 nm) emissive nitrogen-doped CDs based on microwave-assisted pyrolysis of citric acid and ethylenediamine is demonstrated. The duration of

pyrolysis, the molar ratio of acid to amine, and the concentration of reactants were optimized using Central Composite Design and Response Surface Methodology to yield deep red fluorescence. A stock solution citric acid was prepared and the desired amount of this stock solution was added to a glass beaker, then deionized water was added to make the volume and then the desired amount of ethylenediamine was added. The mixture was shaken and heated in a microwave oven for varying durations. MALDI-TOF and DLS results, respectively, showed that as the amine to acid ratio increased, both the MW and size of the CDs increased. On the basis of the XPS analysis, the formation of C–N and the presence of pyrrolic N content appear to be keys to creating red-emissive CDs. Confocal images demonstrated that the nanoparticles could enter the cells, including cancer cells. Excellent biocompatibility results support the potential application of CDs in nanomedicine. Ex vivo porcine eye images showed that intravitreally injected CDs could effectively diffuse through the vitreous to the cornea, and post mortem whole-body mouse images also demonstrated that the CDs are suitable for bioimaging applications. The TEM image displays a snapshot for a size distribution of  $4.05 \pm 0.46$  nm, and the nCDs have a lattice spacing of 0.15 nm. The AFM analysis showed that the particle size of the red-emissive nCDs was less than 5 nm[55].

Jiazhuang Guo et al (2019) synthesized carbon dots (CDs) from green precursors that has received considerable attention recently. They reported the sustainable fabrication of highly fluorescent CDs from food waste, turtle shells, and demonstrate their applications in the fields of multi signal coding and anti-counterfeiting with a combination of colloidal photonic crystals (CPCs). They utilized turtle shells as precursors to synthesize

fluorescent CDs via a simple pyrolysis method. The resultant CDs without further surface treatment have an absolute photoluminescence (PL) QY of 45% and high dispersibility in various solvents. A turtle shell was washed to remove impurities, followed by drying. Then, the dried turtle shell was pulverized into small pieces by a ball mill. Afterward, turtle shell fragments was kept in a tube furnace under nitrogen atmosphere protection. Subsequently, the carbonized product was ground into powder, transferred to deionized water, and then sonicated. Then, the undissolved impurities were removed by centrifugation. The supernatant was filtered and then dialyzed against ultrapure water, followed by freeze drying to yield brownish powder. It was then characterized using Raman spectroscopy, UV-visible spectroscopy, XRD, TEM and FTIR [56].

Zhiguo Ye et al(2020)synthesized the carbon dots with superior antibacterial activity through simple one-step hydrothermal method. In this method, p-phenylenediamine serves as not only the carbon source but also the origin for the functional group anchored on the obtained C-dots. The antibacterial activity of the obtained C-dots was tested against *S. aureus* and *E. coli*. The minimum bactericidal concentration of the synthesized C-dots against *S. aureus* and *E. coli* were 2 and 30  $\mu\text{g/ml}$ , respectively, which are lower than that of these reported C-dots. The antibacterial mechanism was investigated, and the results indicated that a large number of  $-\text{NH}_3^+$  groups on the C-dots surface enhanced their antibacterial activity. Besides, the C-dots exhibited negligible cytotoxicity. The UV-vis absorption spectrum of the C-dots revealed two broad peaks at 245 nm and 285 nm, which originates from the  $\pi$ - $\pi^*$  transition of aromatic  $\text{sp}^2$  domain (C=C and C-C) and  $n$ - $\pi^*$  transition of multi conjugate (C=O and C-O) of C-dots. The TEM images



revealed that prepared C-dots were approximately spherical in shape. The diameter was mostly distributed in 2.5-4.0 nm range with the weighted average of diameter as 3.2 nm. The FT-IR spectra were measured to characterize the functional group on the prepared C-dots. The C-dots and the starting material (p-phenylenediamine) exhibit the similar FT-IR spectra. The X-ray photoelectron spectroscopy (XPS) surveys of the as-prepared C-dots confirmed the FT-IR data[57].

Varsha raveendran et al(2021) proposed, carbon dots derived from Mint leaf extract (M-CDs) via a green method are exploited for versatile applications as a biosensor, reductant, and biomarker. M-CDs are applied for fluorimetric sensing of biologically relevant folic acid through quenching response originating from the inner filter effect, with a limit of detection of 280 nm. It also used as a green reducing agent by demonstrating the reduction of Fe(III) and noble metal nanoparticle synthesis from their salt solutions. Hydrothermal treatment of the leaves under high temperature and pressure leads to dehydration, carbonization, and insitu surface passivation of leaves, which finally leads to the formation of luminescent MCDs. The synthesized MCDs could be used as an effective green reducing agent for ferric ion reduction as well as for the production of stable silver and gold nanoparticles. Transmission electron microscopy was used to study the size distribution and morphology of M-CDs. A single peak in the XRD pattern at  $23.58^\circ$  confirms the graphitic nature.. The Raman spectrum of the M-CDs showed two peaks at 1293 and  $1603\text{ cm}^{-1}$ , which represent the D band and G band, respectively, corresponding to the vibrations of  $sp^3$  and  $sp^2$  carbon atoms. The successful application of a

luminescent material demands high stability. The as-prepared M-CDs show very good fluorescence stability under continuous UV light[58].

## 1.10 OBJECTIVES OF THE WORK

- *Use of crustacean waste, prawns shell waste as a new carbon source for the synthesis of C-dots by hydrothermal method.*
- *Characterization of synthesized C-dots using various analytical techniques like*

*FT-IR*

*UV- Visible spectroscopy*

*Fluorescence study*

*TEM*

- *To Study the antibacterial activity of synthesized C-dots.*
- *Preparation and characterization of C-dot-Zinc Oxide nanocomposite and Copper doped Zinc Oxide-C-dot nanocomposite.*
- *Conduct a comparative study of the antibacterial activity of these composites with C-dot.*

## Chapter 2

### **MATERIALS AND METHOD**

#### **2.1 CHARACTERIZATION TECHNIQUES**

A wide range of characterization techniques are currently being employed to study the morphology (i.e., size, shape, and structure), topography, elemental composition, crystallographic information, size distribution, and granular orientation of various types of CDs prepared through different synthetic methods. These methods principally include the microscopy, spectrometry, spectroscopy, as well as the diffraction techniques. Mostly CDs are characterized by microscopies such as transmission electron microscopy (TEM), and scanning electron microscopy (SEM). Various spectroscopic techniques such as Ultra Violet-visible (UV-Vis), Fourier transfer infrared (FTIR), have also been used for the characterization of CDs[59].

##### **2.1.1 FOURIER-TRANSFORMED INFRARED SPECTROSCOPY (FTIR)**

FTIR is a technique based on the measurement of the absorption of electromagnetic radiation with wavelengths within the mid-infrared region (4000-400  $\text{cm}^{-1}$ ). If a molecule absorbs IR radiation, the dipole moment is

somehow modified and the molecule becomes IR active. A recorded spectrum gives the position of bands related to the strength and nature of bonds, and specific functional groups, providing thus information concerning molecular structures and interactions. Attenuated total reflection (ATR) is a sampling technique used alongside traditional infrared spectroscopy, which ultimately qualifies samples to be observed directly in either solid or liquid state, without additional preparation. An attenuated total reflection accessory functions by quantifying the changes that happen to an internally-reflected infrared beam, once it comes into contact with the chosen sample. To do this, an infrared beam is focused onto a crystal with a high refractive index at a set angle. The resulting internal reflections create a transient wave that reaches beyond the outer surface of the optically dense crystal, and then into the sample which is held in contact with it. This initial wave only protrudes by a couple of microns (between 0.5  $\mu$  and 5  $\mu$ ) beyond the surface of the crystal, and into the sample itself. Therefore, there must be decent contact made between the chosen sample and the surface of the crystal. In the parts of the spectrum where the sample absorbs energy, the wave will be either altered or attenuated [60].

### **2.1.2 TRANSMISSION ELECTRON MICROSCOPY(TEM)**

TEM is a microscopy technique that exploits the interaction between a uniform current density electron beam (i.e. the energies are usually within a range of 60 to 150 keV) and a thin sample. TEM retrieves the chemical information and the images of CDs at a spatial resolution equal to the level of atomic dimensions. In TEM, the electron beam through which an incident light is transmitted via a thin foil specimen and transformed into

elastically or inelastically scattered electrons, when the electron beam interacts with the sample of CDs. Precise particle size of bright field images as well as dark field images are provided by the TEM, and it gives details about the morphology, composition, and crystallographic information of CDs as it utilizes energetic electrons. Nowadays, high resolution TEM (HRTEM) is broadly employed for studying the lattice and surface imperfections of CDs. The size and morphology define the unique set of physical properties, such as optical magnetic, electronic and catalytic of NPs, as well as their interaction with biological systems. TEM is the most common technique to analyse nanoparticle size and shape, since it provides not only direct images of the sample but the most accurate estimation of the nanoparticle homogeneity. TEM instruments have multiple operating modes including conventional imaging, scanning TEM imaging (STEM), diffraction, spectroscopy, and combinations of these. TEM is capable of returning an extraordinary variety of nanometer- and atomic-resolution information, in ideal cases revealing not only where all the atoms are but what kinds of atoms they are and how they are bonded to each other. For this reason TEM is regarded as an essential tool for nanoscience in both biological and materials fields [61].

### **2.1.3 UV-VISIBLE SPECTROSCOPY(UV-Vis)**

UV spectroscopy or UV-visible spectrophotometry (UV-Vis or UV/Vis) refers to absorption spectroscopy or reflectance spectroscopy in part of the ultraviolet and the full, adjacent visible regions of the electromagnetic spectrum. This means it uses light in the visible and adjacent ranges. The absorbance or reflectance in the visible range directly affects the perceived

colour of the chemicals involved. In this region of the electromagnetic spectrum, atoms and molecules undergo electronic transitions. Absorption spectroscopy is complementary to fluorescence spectroscopy. Molecules containing electrons or nonbonding electrons(n) can absorb energy in the form of UV or Visible light to excite these electrons to higher antibonding molecular orbitals. The more easily excite the electrons the longer the wavelength of light it can absorb. This spectroscopy is routinely used in analytical chemistry for the quantitative determination of different analytes such as transition metal ions, highly conjugated organic compounds and biological macromolecules. For instance, solutions of transition metal ions can be coloured because d-electrons within the metal atoms can be excited from one electron state to another. The colour of the metal ion solutions is strongly affected by the presence of the ligands. The instrument in the UV-Visible spectroscopy is called UV-Visible spectrophotometer. It measures the intensity of light passing through a sample (I) and compares it to the intensity of light before it passes through the sample (I<sub>0</sub>). The ratio I/I<sub>0</sub> are called transmittance and are usually expressed as a percentage (%T). The absorbance A is based on transmittance [62].

$$A = -\log (\%T/100\%)$$

#### **2.1.4 X-RAY DIFFRACTION(XRD)**

X-ray diffraction (XRD) is one of the most extensively used techniques for the characterization of nanoparticles. Typically, XRD provides information regarding the crystalline structure, nature of the phase, lattice parameters and crystalline grain size. When a crystal with an interplanar spacing *d* (crystal lattice constant) is irradiated by X-ray beam with a

comparable wavelength  $\lambda$ , the X-ray diffraction or the constructive interference between elastically scattered X-ray beams can be observed at specific angles  $2\theta$  when the Bragg's Law is satisfied,  $n\lambda = 2d\sin\theta$  where  $n$  is any integer. Samples are often prepared as smear or compact flat or in capillary and are exposed to a monochromatic beam of X-ray which is diffracted by the nanomaterial and data on the diffracted beam is collected at an angle ( $2\theta$ ) with respect to the incident beam. A powder diffraction pattern supplies information from the nanomaterial on phases present, phase concentrations, structure, as well as the degree of crystallinity or amorphous content followed by details on crystallite size/strain. The peak widths in given phase pattern provides information on the average crystallite size where large crystallites give rise to sharp peaks and any increase in the peak width indicates a reduced crystallite size. The particle size of the crystal is estimated by using Scherrer's equation. An advantage of the XRD techniques, commonly performed in samples of powder form. The broadening of XRD peaks was mainly caused by particle/crystallite size and lattice strains other than instrumental broadening[63].

#### **2.1.5 SCANNING ELECTRON MICROSCOPE(SEM)**

SEM is one of the most widely used techniques used in characterization of nanomaterials and nanostructures. The signals that derive from electron-sample interactions reveal information about the sample including surface morphology (texture), chemical composition of the sample. Accelerated electron in a SEM carry significant amounts of kinetic energy. This energy is dissipated as a variety of signals produced by electron - sample interaction when the incident electrons are decelerated in solid sample. Due to very narrow electron beams, SEM micrographs have a large depth of

field yielding a characteristic three dimensional appearance useful for understanding the surface structure of the sample. When electron beam comes and hits the atoms of specimen those atoms absorb their energy and give off their own electron- secondary electron. There is a detector to pick up the secondary electron which has a positive charge on it about 300 V. Secondary Electrons (SE) are emitted from very close to specimen surface and can produce very high resolution image of sample surface revealing details less than 1nm. The electron beam is generally scanned in a raster pattern and the beam's position is combined with the detected signal to produce an image of the surface. SEM requires more time-consuming sample preparation. The information obtained is visual and descriptive, it is usually not quantitative since only a few particles are seen in the viewing field at one time. However, when SEM is used with other techniques such as laser diffraction, it can provide valuable additional information on particle texture, which may help to explain agglomeration or flow problems[64].

#### **2.1.6 ENERGY DISPERSIVE X-RAY ANALYSIS(EDAX)**

EDX referred to as EDS or EDAX, is an X-ray technique used to identify the elemental composition of materials. EDX systems are attachments to Electron Microscopy instruments (Scanning Electron Microscopy (SEM) or Transmission Electron Microscopy (TEM)) instruments where the imaging capability of the microscope identifies the specimen of interest. The basic principle of EDAX is a generation of X-rays from a specimen through the electron beam . To produce characteristic X-rays from an object, it is bombarded by either a highly energetic beam of charge carriers (electrons or protons) or X-rays. The atoms of the sample contain ground state



(unexcited) electrons in discrete energy levels or electron shells bound to the nucleus. An electron from an inner shell may be excited by an incident beam, thereby removing it from its shell and generating a hole where electron was present before excitation. This hole can be occupied by an electron of a higher-energy shell. The difference in energies of the higher- and lower- energy shells is emitted as an X-ray. Quantitative measurement of the energy and number of these X-rays can be done with energy-dispersive analysis of X-rays. Since the energy of these X-rays is characteristic feature of energy difference between two shells and atomic structure of discharging element, EDAX can be employed to identify the elemental composition of an object. The data generated by EDAX analysis consist of spectra showing peaks corresponding to the elements making up the true composition of the sample being analysed. Elemental mapping of a sample and image analysis are also possible. Applications include materials and product research, troubleshooting, de-formulation, and more [65].

## **2.2 SYNTHESIS OF CARBON DOT**

### **2.2.1 MATERIALS**

- Powdered prawns shell
- 3% NaOH
- 1% HCl
- 50% NaOH
- 2% Acetic acid

### **2.2.2 METHOD**

#### **SAMPLE COLLECTION AND PRETREATMENT**

Prawn shells were collected from house hold wastes. The prawn shell was washed with water and dried in day light for one week. The dried shells were ground by using mixer grinder to make the fine powder. +The powdered prawn shells were again washed with distilled water. The cleaned samples were dried overnight at 80 °C[66].

#### **SYNTHESIS OF CARBON DOTS**

2.0 g of dried prawn shell powder was treated with 25 mL of 3% NaOH solution at room temperature for 5 h. The powder washed with deionized water followed by centrifugation until a neutral pH was obtained. The sample was treated with 1% hydrochloric acid solution for 6 h at room temperature. After acid treatment, the sample was washed with deionized water and centrifuged several times to obtain a neutral pH. The prawn shells were transferred to a 50% sodium hydroxide solution and refluxed at 80°C for 2 h. The refluxed sample was cooled down to the room temperature and filtered through Whatman filter paper. The obtained product was dispersed in 25 mL of 2% acetic acid solution. Then the sample was transferred to 45 mL capacity stainless steel autoclave and kept at 200°C for 8 h. The C-dots were collected by removing the large particles through centrifugation at 4,000 rpm for one hour followed by suction filtration using polyvinylidene difluoride (PVDF) membrane. The sample were used for further characterization purpose [66].

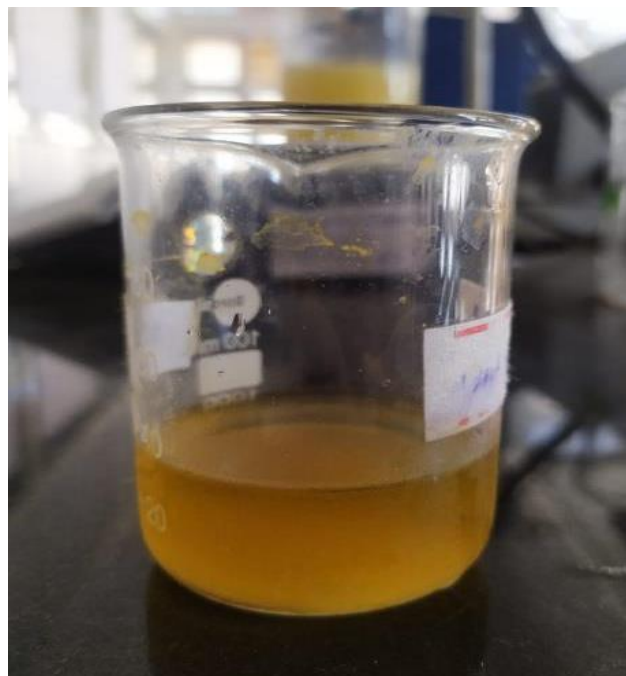


Fig 2.1: synthesized carbon dot

## **2.3 SYNTHESIS OF ZINC OXIDE NANOPARTICLE FROM ZINC ACETATE**

### **2.3.1 MATERIALS**

- Zinc Acetate (0.1M)
- NaOH (0.1M)

### **2.3.2 METHOD**

Zinc acetate and sodium hydroxide were used as precursors. Zinc oxide nanoparticles were synthesized through precipitation method. To the aqueous solutions of zinc acetate (0.1 M) sodium hydroxide solution (0.1

M) was added slowly in drops (0.5 ml/min), under vigorous stirring. The reaction was kept overnight for stabilization. It was then centrifuged at 6000 rpm for 25 minutes and washed with distilled water. The nanoparticles were dried in an oven at 60°C for 14 h, for the complete removal of solvent and any volatile impurities. After drying nanoparticles, were ignited in a muffle furnace at 500°C for 15–20 min. The ignited NPs were stored under airtight conditions[67].

## **2.4 SYNTHESIS OF COPPER DOPED ZINC OXIDE NANOPARTICLE**

### **2.4.1 MATERIALS**

- Zinc Nitrate Hexahydrate (0.9M)
- Copper Nitrate Hexahydrate (0.1M)
- Potassium Hydroxide (5M)

### **2.4.2 METHOD**

Cu-doped ZnO nanoparticles were synthesized using the co-precipitation process. 200 ml of an aqueous mixture of zinc nitrate and copper nitrate was used at Cu:Zn molar ratio of 1:9 for 10% Cu doped ZnO. An aqueous KOH (5M) was slowly dropped into the mixture solution while stirring with a magnetic stirrer until the pH value reached 14. Precipitate formed in the solution was kept overnight. After that, the precipitate was washed with distilled water and centrifuged at 6000 rpm for 20 minutes. Then the precipitate was dried in an oven at 120<sup>0</sup> C for 12 hours [68].



# Chapter 3

## **RESULTS AND DISCUSSION**

### **3.1 CHARACTERIZATION OF CARBON DOT**

#### **3.1.1 FT-IR STUDIES**

Fourier transform infrared (FTIR) spectroscopy was conducted in order to study the surface groups, structure of the C-dot(Fig 3.1). It show the chemical bonding in a sample through absorption of Infrared radiation. The strong band at 3400– 3100  $\text{cm}^{-1}$  which could be due to either –OH or –NH stretching of surface functionalities. A weak band observed at 2200–2000  $\text{cm}^{-1}$  may be attributed to the presence of nitrile group. The strong absorption band at 1550–1650  $\text{cm}^{-1}$  indicates the presence –NH<sub>2</sub> group through amide (–C=O) bonds. However, other groups contributed to the absorption in this region including C=C vibrations of aromatic compounds, non-aromatic double bonds, hydrogen bonds of the C=O groups of ketone and the symmetric stretching of the COO<sup>-</sup> group. The absorption at 1412  $\text{cm}^{-1}$  can be attributed to the symmetrical deformations of CH<sub>3</sub> group. The existence of –C–O–C was also identified from the narrow band obtained at 1018  $\text{cm}^{-1}$ [69].

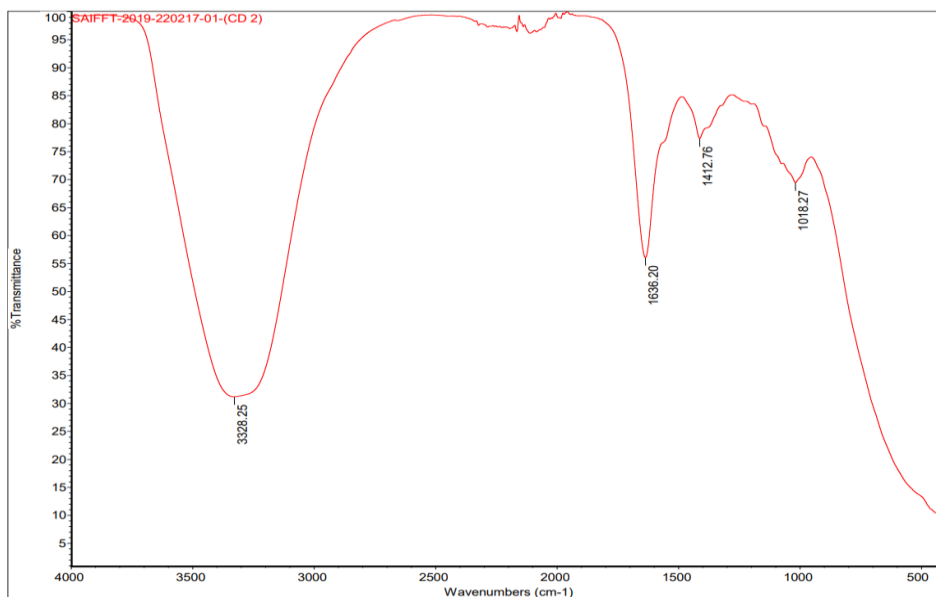


Fig 3.1 : FT-IR spectrum of synthesized C-dot

Table 3.1 : FTIR peaks of Carbon dot

3400-3100 cm <sup>-1</sup>	N-H or O-H stretching
2200-2000 cm <sup>-1</sup>	nitrile group
1550-1650 cm <sup>-1</sup>	presence of NH <sub>2</sub> through amide
1412 cm <sup>-1</sup>	symmetric stretching vibration of COO-
1018 cm <sup>-1</sup>	out of plane O-H bending

### 3.1.2 UV-VISIBLE SPECTROSCOPY

The fluorescent C-dots were inspected using UV-Vis spectroscopy. From the UV-Vis spectra (Fig 3.2), it can be seen that there are two absorption peaks, one at 280 nm (sharpen absorption peak) and another around 330 nm (flat). These peaks are obtained due to  $\pi \rightarrow \pi^*$  and  $n \rightarrow \pi^*$  electronic transition in C-dots surface [66].

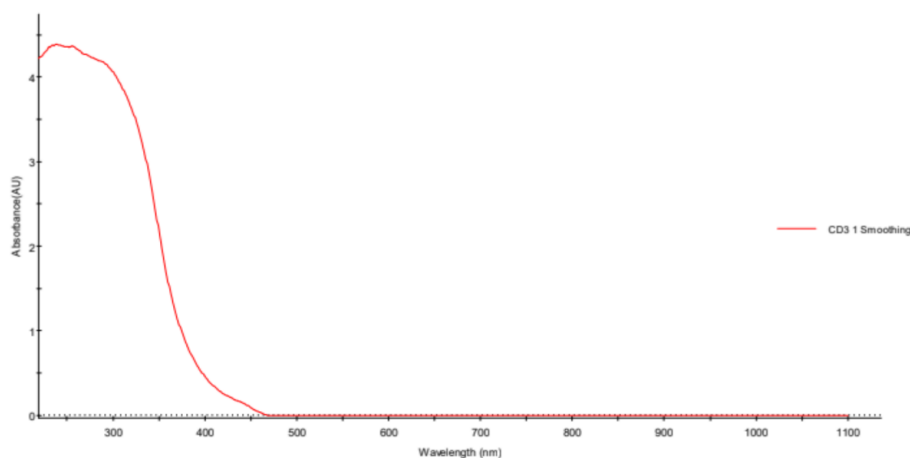


Fig 3.2 : UV-Vis spectrum of synthesized carbon dot

### 3.1.3 FLUORESCENCE STUDY

The prepared C-dot solution was yellowish in color under normal light and exhibited intense green fluorescence under UV excitation (Fig 3.3(a)). The intensity of the green fluorescence was observed to diminish with time. This is due to the instability of synthesized carbon dot. Fig 3.3(b) and Fig 3.3(c) shows the decrease in fluorescent intensity on storage.



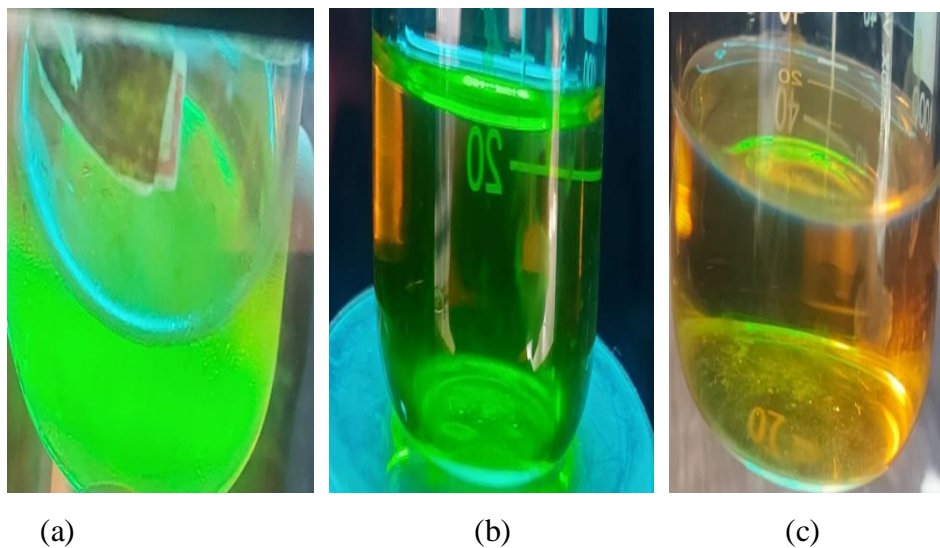
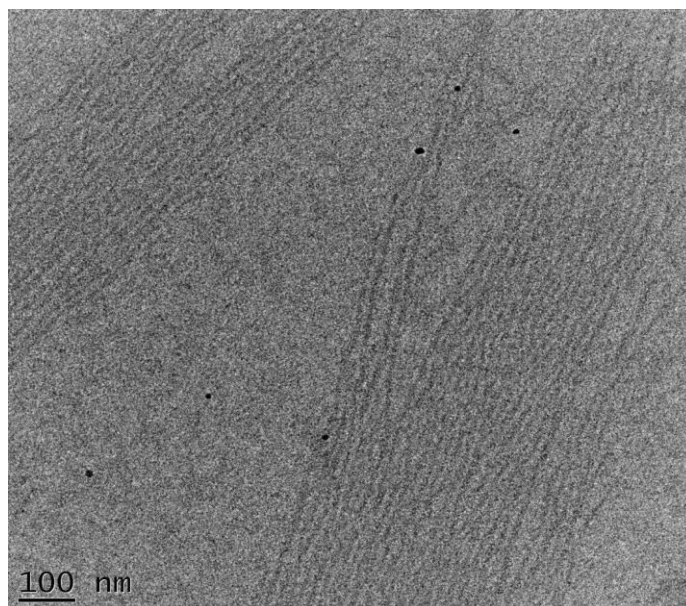


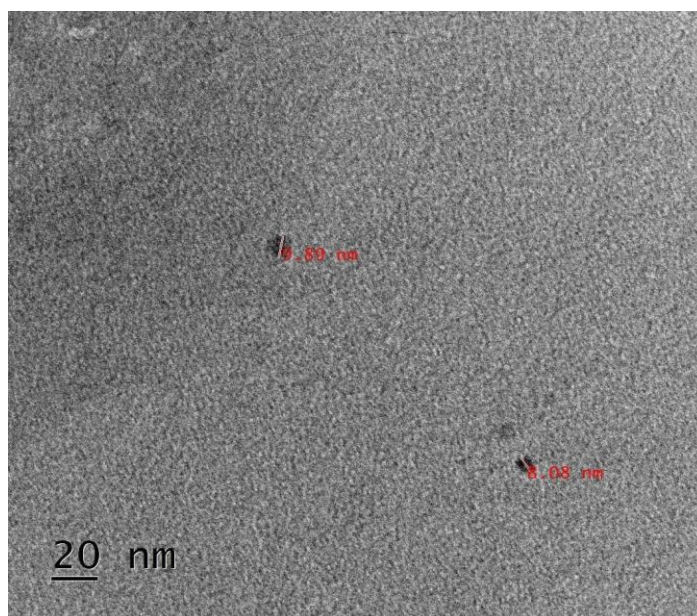
Fig 3.3 : fluorescent carbon dot excited by UV light.

### **3.1.4 TEM**

Transmission electron microscopes (TEM) studies were conducted in order to examine the morphology, size, nature and chemical composition of synthesized carbon dot. The TEM images of C-dots reveal that the C-dots are homogeneous, and particles are dispersed in a spherical shape (Fig 3.4 (a)). The resulting C-dots diameter ranges from 8 to 9 nm (Fig 3.4 (b)).



(a)



(b)

Fig 3.4 : TEM images of the synthesized carbon dot

## 3.2. CHARACTERIZATION OF ZINC OXIDE NANOPARTICLES

### 3.2.1 X-RAY DIFFRACTION

The crystal sizes of ZnO nanoparticles was analyzed using XRD studies. Figure 3.5 shows the XRD spectrum of synthesized ZnO nanoparticles. In the XRD spectrum of ZnO nanoparticles from zinc acetate five clear peaks were observed. The average crystal size was determined using Debye Scherrer equation,

$$D = 0.9 \lambda / B \cos \theta$$

Where B is the full width at half maximum (FWHM) and  $\theta$  is the angle of the maximum peak and  $\lambda$  is the wavelength of the source. The average crystal size was found to be 13.252 nm. This confirms that the particles belongs to nano range (Refer table 3.2).

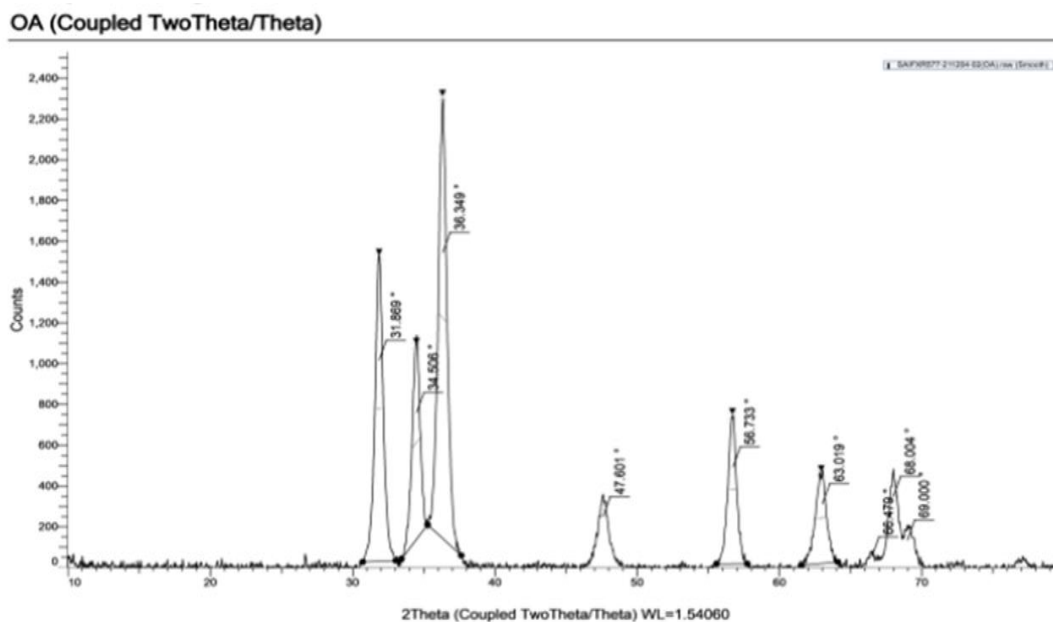


Fig 3.5 : XRD spectrum of zinc oxide nanoparticles

**Analysis of peaks:**

**Peak 1**

$$2\theta = 31.7^\circ$$

$$\theta = 15.93^\circ = 0.2780 \text{ radian}$$

$$B = 0.598 = 0.01043 \text{ radian}$$

$$\lambda = 1.54060 \times 10^{-10}$$

From Debye Scherrer equation ,

$$\begin{aligned} D &= 0.9 \lambda / B \cos \theta = 0.9 \times 1.54060 \times 10^{-10} / 0.01043 \cos 0.2780 \\ &= 13.815 \text{ nm} \end{aligned}$$

**Peak 2**

$$2\theta = 34.476^\circ$$

$$\theta = 17.238^\circ = 0.3009 \text{ radian}$$

$$B = 0.612 = 0.0107 \text{ radian}$$

$$\lambda = 1.54060 \times 10^{-10}$$

From Debye Scherrer equation ,

$$\begin{aligned} D &= 0.9 \lambda / B \cos \theta = 0.9 \times 1.54060 \times 10^{-10} / 0.0107 \cos 0.3009 \\ &= 13.5679 \text{ nm} \end{aligned}$$

**Peak 3**

$$2\theta = 36.333^\circ$$

$$\theta = 18.16665^\circ = 0.3171 \text{ radian}$$

$$B = 0.632 = 0.01103 \text{ radian}$$

$$\lambda = 1.54060 \times 10^{-10}$$

From Debye Scherrer equation ,

$$\begin{aligned} D &= 0.9 \lambda / B \cos \theta = 0.9 \times 1.54060 \times 10^{-10} / 0.01103 \cos 0.3171 \\ &= 13.2290 \text{ nm} \end{aligned}$$

#### **Peak 4**

$$2\theta = 56.689^\circ$$

$$\theta = 28.3445^\circ = 0.4947 \text{ radian}$$

$$B = 0.626 = 0.0109 \text{ radian}$$

$$\lambda = 1.54060 \times 10^{-10}$$

From Debye Scherrer equation ,

$$\begin{aligned} D &= 0.9 \lambda / B \cos \theta = 0.9 \times 1.54060 \times 10^{-10} / 0.0109 \cos 0.4947 \\ &= 14.4200 \text{ nm} \end{aligned}$$

#### **Peak 5**

$$2\theta = 62.920^\circ$$

$$\theta = 31.451^\circ = 0.5489 \text{ radian}$$

$$B = 0.831 = 0.0145 \text{ radian}$$

$$\lambda = 1.54060 \times 10^{-10}$$

From Debye Scherrer equation ,

$$D = 0.9 \lambda / B \cos \theta = 0.9 \times 1.54060 \times 10^{-10} / 0.0145 \cos 0.5489$$

$$= 11.208 \text{ nm}$$

Table 3.2 : Average particle size of Zinc Oxide nanoparticles from Zinc Acetate

2 $\theta$ of the intense peak(deg)	FWHM of intense peak	Size of particle, D, (nm)	Average particle size (nm)
31.867 <sup>0</sup>	0.598	13.815	13.247
34.476 <sup>0</sup>	0.612	13.5679	
36.333 <sup>0</sup>	0.632	13.229	
56.689	0.62	14.420	
62.902 <sup>0</sup>	0.831	11.208	

### 3.2.2 FT-IR STUDIES

FT-IR was performed in order to study and determine the functional groups of synthesized ZnO nanoparticles prepared from Zinc Acetate. Figure 3.6 shows the FTIR spectrum of the prepared ZnO nanoparticles. FTIR spectral studies reveals the chemical bonding between Zinc and Oxygen. The peak at 425.32 cm<sup>-1</sup> is the characteristic absorption of Zn-O bond (ZnO stretching vibration) and the broad absorption peak at 3426 cm<sup>-1</sup> can be attributed to the characteristic absorption of hydroxyl group. The peaks at

1384.43  $\text{cm}^{-1}$  and 1628.72  $\text{cm}^{-1}$  are symmetric and asymmetric O-C-O stretching vibration of adsorbed carbonate anion respectively [70].

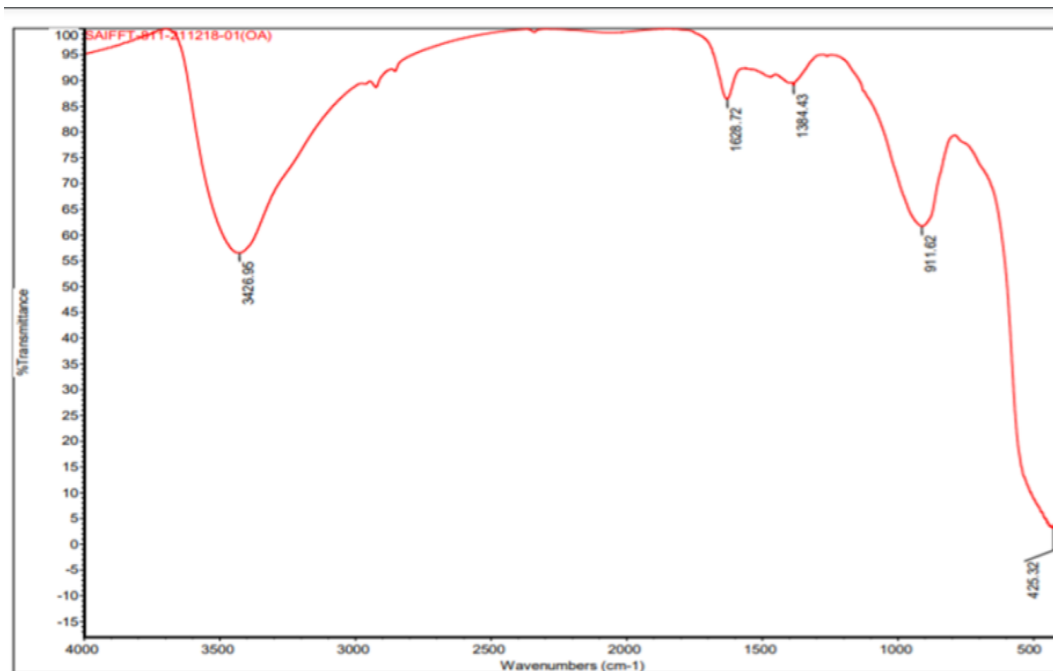


Fig 3.6 : FT-IR spectrum of zinc oxide nanoparticle

Table 3.3 : FTIR peak assignments of Zinc Oxide nanoparticles from Zinc Acetate

425.32 $\text{cm}^{-1}$	Zn-O bond
3426 $\text{cm}^{-1}$	absorption of hydroxyl.
1384.43 $\text{cm}^{-1}$ and 1628.72 $\text{cm}^{-1}$	symmetric and asymmetric O-C-O stretching vibration of adsorbed carbonate anion respectively

### **3.2.3 SEM**

SEM studies was carried out in order to examine the morphology of the prepared ZnO nano powder. The SEM image of the obtained ZnO nano powder is shown in Figure 3.7.

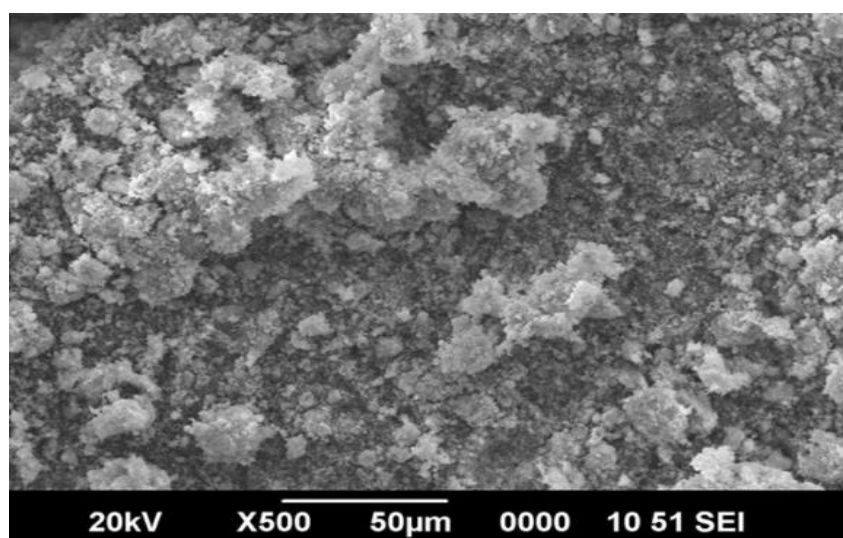


Fig 3.7 : SEM image of synthesized Zinc Oxide nanoparticles from Zinc Acetate

### **3.2.4 EDAX**

EDAX studies was done in order to determine the elemental composition of the samples. Figure 3.8 shows the EDAX spectrum of the synthesized ZnO nanoparticles. Spectrum shows the presence of two elements which are Zinc and Oxygen. Thus, the EDAX result revealed that the synthesized ZnO NPs were of high purity, which contain high Zinc and Oxygen elemental composition [71].



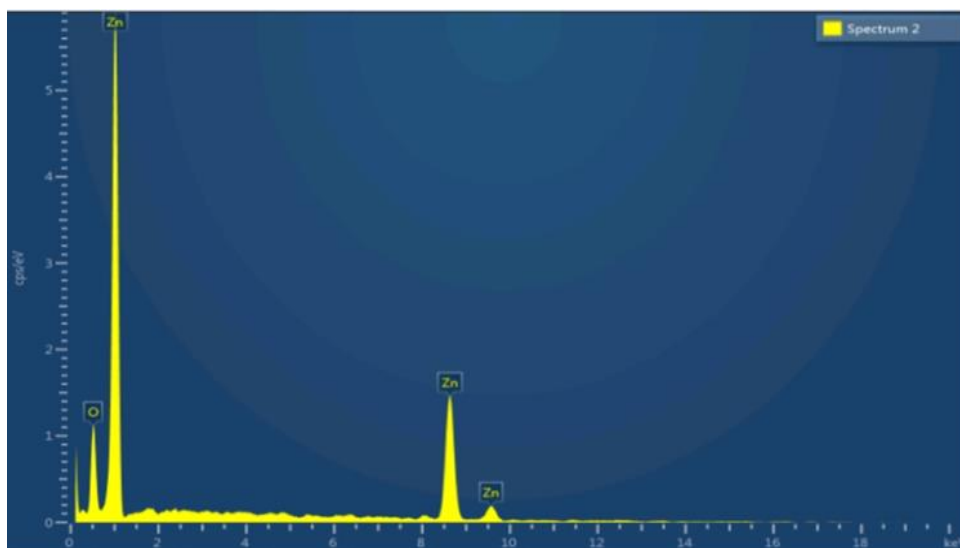


Fig 3.8: EDAX spectrum of Zinc Oxide nanoparticles

### 3.3 CHARACTERIZATION OF COPPER DOPED ZINC OXIDE NANOPARTICLES

#### 3.3.1 X-RAY DIFFRACTION

Figure 13. shows the XRD patterns of 10 % Copper doped Zinc Oxide. In the XRD spectrum an extra peak was observed at  $38.447^\circ$  as compared to undoped ZnO XRD pattern. This indicates that the copper is doped into the ZnO lattice. In the XRD spectrum four clear peaks were observed. The average crystal size was determined using Debye Scherrer equation,

$$D = 0.9\lambda/\beta \cos \theta$$

The average crystal size was found to be 23.6278 nm.

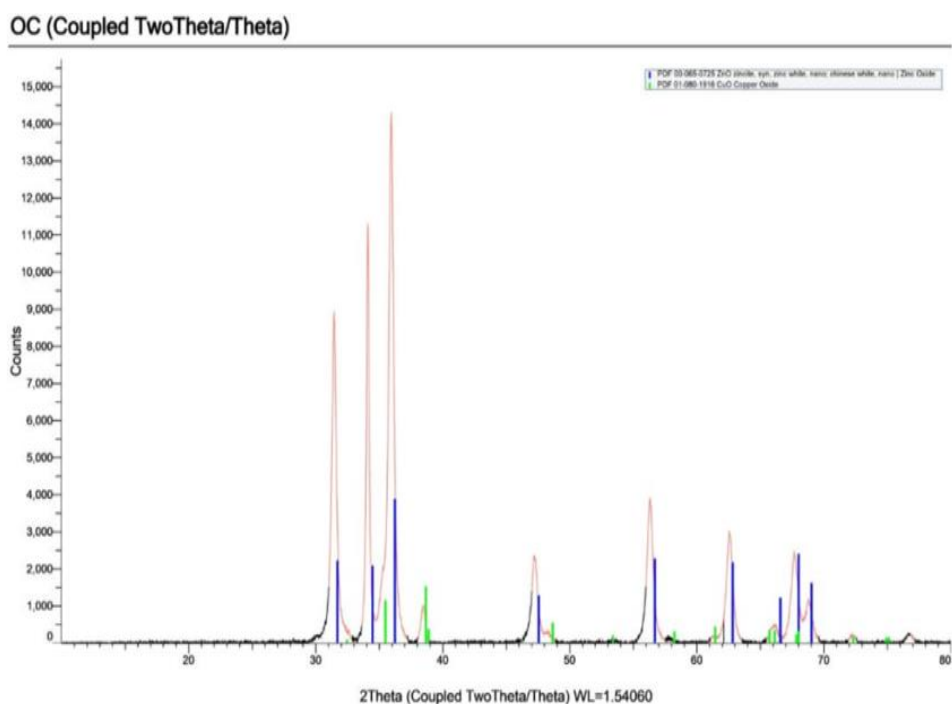


Fig 3.9 : XRD spectrum of synthesized Copper doped Zinc Oxide nanoparticles

### Analysis of peaks:

#### Peak 1

$$2\theta = 31.444^\circ$$

$$\theta = 15.722^\circ = 0.274 \text{ radian}$$

$$\beta = 0.403 = 0.00703 \text{ radian}$$

$$\lambda = 1.5406 \times 10^{-10} \text{ m}$$

From Debye Scherrer equation,

$$D = 0.9\lambda/\beta \cos \theta$$

$$= 0.9 \times 1.5406 \times 10^{-10} / 0.00703 \times \cos(0.274) = 20.4897 \text{ nm}$$

**Peak 2**

$$2\theta = 34.099^\circ$$

$$\theta = 17.049^\circ = 0.297 \text{ radian}$$

$$\beta = 0.236 = 0.0041 \text{ radian}$$

$$\lambda = 1.5406 \times 10^{-10} \text{ m}$$

From Debye Scherrer equation,

$$D = 0.9\lambda/\beta \cos \theta$$

$$= 0.9 \times 1.5406 \times 10^{-10} / 0.0041 \times \cos(0.297) = 35.2000 \text{ nm}$$

**Peak 3**

$$2\theta = 35.948^\circ$$

$$\theta = 17.974^\circ = 0.3137 \text{ radian}$$

$$\beta = 0.395 = 0.0069 \text{ radian}$$

$$\lambda = 1.5406 \times 10^{-10} \text{ m}$$

From Debye Scherrer equation,

$$D = 0.9\lambda/\beta \cos \theta$$

$$= 0.9 \times 1.5406 \times 10^{-10} / 0.0069 \times \cos(0.3137) = 21.1156 \text{ nm}$$

**Peak 4**

$$2\theta = 56.315^\circ$$

$$\theta = 28.1575^\circ = 0.4914 \text{ radian}$$

$$\beta = 0.509 = 0.0089 \text{ radian}$$

$$\lambda = 1.5406 \times 10^{-10} \text{ m}$$

From Debye Scherrer equation,

$$D = 0.9\lambda/\beta \cos \theta$$

$$= 0.9 \times 1.5406 \times 10^{-10} / 0.0089 \times \cos 0.4914 = 17.7059 \text{ nm}$$

Table 3.4: Average particle size of copper doped Zinc Oxide nanoparticles

2 $\theta$ of the intense peak(deg)	FWHM of intense peak	Size of particle, D (nm)	Average particle size (nm)
31.444	0.403	20.4897	23.6278
34.099	0.236	35.2000	
35.948	0.395	21.1156	
56.315	0.509	17.7059	

### 3.3.2 FT-IR STUDIES

FT-IR Spectroscopy was employed to study the influence of Cu doping on Zn–O bonding. Figure 3.10 shows the FT-IR spectrum of synthesized Copper doped ZnO nanoparticles. FT-IR spectra has been recorded in the range 4000–400  $\text{cm}^{-1}$ . A band was observed between 400 - 500 $\text{cm}^{-1}$  for the pure ZnO corresponding to the formation of Zn–O bond. The absorption peaks at 3379 and 1380  $\text{cm}^{-1}$  are attributed to O–H stretching of H<sub>2</sub>O. The band at 893  $\text{cm}^{-1}$  is assigned to the vibrational frequencies due to the change in the microstructural features by the addition of Copper into Zn–O lattice [72].

Fig 3.10 : FT-IR spectrum of synthesized Copper doped Zinc Oxide nanoparticles

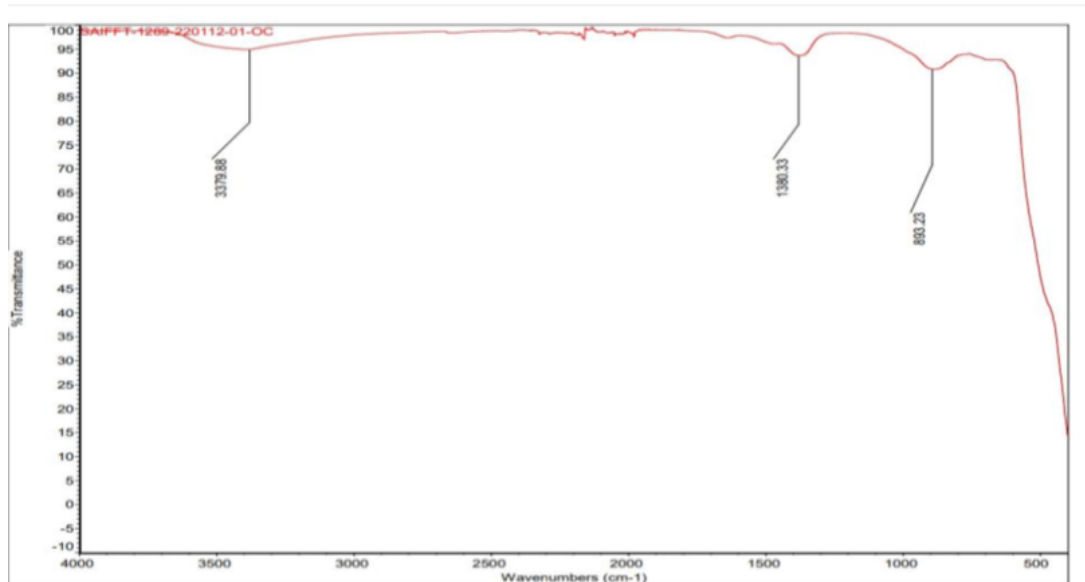


Table 3.5: FTIR peaks of Copper doped Zinc Oxide nanoparticles

400-500cm <sup>-1</sup>	Zn-O bond
3379cm <sup>-1</sup>	O-H stretching of H <sub>2</sub> O
1380cm <sup>-1</sup>	O-H stretching of H <sub>2</sub> O
893cm <sup>-1</sup>	Cu in Zn-O lattice

### 3.3.3 SEM

SEM studies were conducted in order to examine the morphology of the prepared ZnO nano powder. The SEM images of Copper doped ZnO nano powder is shown in Figure 3.11. There is a remarkable morphology change

in the shape and particle size due to the incorporation of  $\text{Cu}^{2+}$  into  $\text{Zn}^{2+}$  sites. Particles are more scattered and aggregates are formed as compared to undoped ZnO.

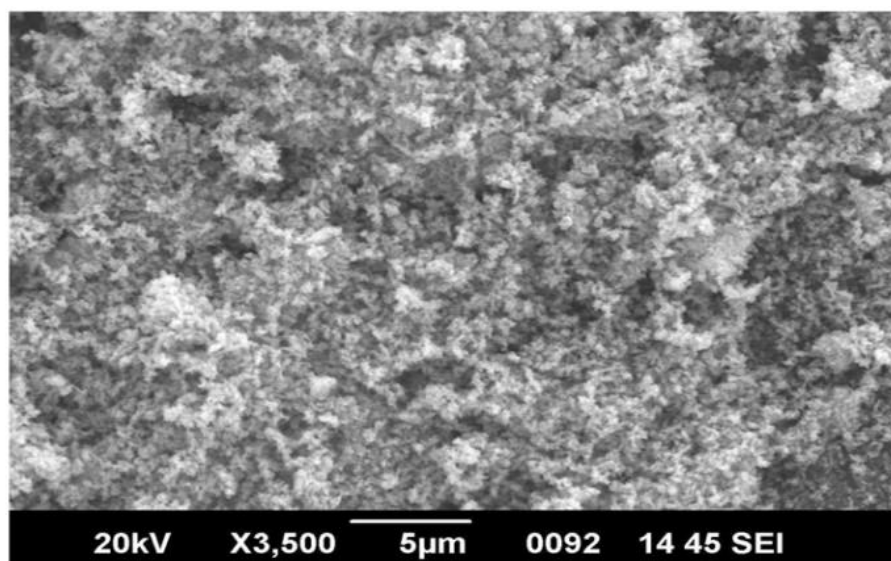


Fig 3.11: SEM image of synthesized Copper doped Zinc Oxide nanoparticles

### 3.3.4 EDAX

EDAX was used in order to determine the elemental composition present in the sample. Figure 3.12 shows the EDAX spectrum of the synthesized Copper doped Zinc Oxide nanoparticles. Spectrum shows the presence of three elements which are Zinc, Oxygen and Copper. Thus, the EDAX result revealed that the synthesized Copper doped Zinc Oxide nanoparticles were of high purity, which contain Copper in addition to Zinc and Oxygen of undoped ZnO nanoparticles [73].

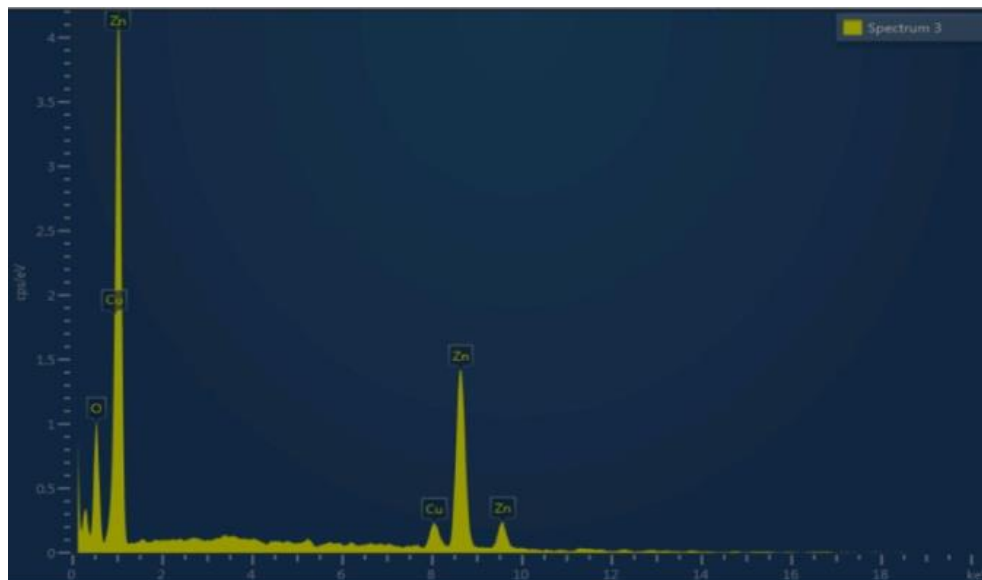


Fig 3.12 : EDAX spectrum of synthesized Copper doped Zinc Oxide nanoparticles

### 3.4 ANTIBACTERIAL STUDY OF CARBON DOT AND ITS NANOCOMPOSITE

#### 3.4.1 SYNTHESIS OF C-DOT-ZINC OXIDE NANOCOMPOSITE

0.1g of synthesized ZnO was dissolved in 20 ml solution of previously prepared CDs and stirred for 15 min at room temperature, then transferred into the autoclave to react for 3 hr at 100<sup>0</sup>C. The obtained nanocomposite were used for further studies [74].

### **3.4.2 SYNTHESIS OF COPPER DOPED ZINC OXIDE - C-DOT NANOCOMPOSITE**

0.1g of synthesized Cu-doped ZnO nanoparticle was dissolved in 20 ml solution of previously prepared CDs and stirred for 15 min at room temperature, then transferred into the autoclave to react for 3 hr at 100°C. The obtained composite was used for further studies.

### **3.4.3 ANTIBACTERIAL ACTIVITY ASSAY**

The antibacterial activities of the C-dot, C-dot-ZnO nanocomposite and Cu doped ZnO-C-dot nanocomposite were assessed by agar well diffusion method. One ml of the fresh culture of *E.Coli* and *Staphylococcus* was inoculated in the sterile Petri dishes distinctly. Wells were made using a sterile cork borer into agar plates containing inoculums. Then, 100 µl of each test solution was added to respective wells. The test solutions were C-dot(D), C-dot-ZnO(E) and Copper doped ZnO-C-dot(F). Then, the plates were incubated at 37°C for 24 hours. Antimicrobial activity was detected by measuring the zone of inhibition (including the diameter of the wells) that appeared after the incubation period. Acetic acid was employed as a negative control. Tetracycline, an antibiotic was used as the standard.





(a)



(b)

Fig 3.13: images of *S. aureus*(a) and *E. coli* (b) bacteria after incubation

After incubation for 24 hours, it has been found that C-dot is bacteriosidal against both *E.Coli* and *S.aureus* . C-dot is showing the diameter of a zone of inhibition of 1cm against both the bacterial strains. For C-dot-ZnO nanocomposite, the diameter of zone of inhibition for E.coli became 1.5 cm whereas for *S.aureus* it became 1.2 cm. Therefore C-dot-ZnO nanocomposite shows more antibacterial activity against *E.coli*.

Cu doped ZnO-C-dot nanocomposite exhibited enhanced antibacterial activity than both C-dot and C-dot-ZnO nanocomposite. Therefore it can be concluded that the antibacterial activity of C-dot can be enhanced by the preparation of their nanocomposites with ZnO and Cu doped ZnO.

Table 3.6 : Comparative study of antibacterial activity

SAMPLE	DIAMETER OF ZONE OF INHIBITION	
	E.coli	S.aureus
D) C- DOT	1 cm	1 cm
E) C-dot-ZnO nanocomposite	1.5 cm	1.2 cm
F) Cu doped ZnO-C-dot	1.7 cm	1.3 cm

## Chapter 4

### 4.1 CONCLUSIONS

Every year, 6 million to 8 million tones of crustacean wastes are produced globally; about 1.5 million tones in south east Asia alone. In developing countries, waste shells are often just dumped in landfill or the sea. In developed countries, disposal methods can be costly. The improper disposal of these wastes can cause negative impacts on both human health as well as environment. Crustacean shells constitute 20–40% protein, 20–50% calcium carbonate and 15–40% chitin. Chitin and its derivatives are widely used in innumerable application ranging from food, agriculture, biomedicine, pharmaceuticals etc. Therefore, the extraction of chitin from crustacean shells and its use as is or after further processing may be a way to minimize the waste and to produce valuable compounds with remarkable biological properties and crucial application in various fields. The main objective of this work is to explain the utilization of crustacean wastes in a productive manner such that it would offer environment and economic sustainability.

In this work we have focused on the synthesis, characterization and application studies of fluorescent carbon dot from prawn shell waste by hydrothermal method. The synthesized carbon dot was characterized using XRD, TEM, and UV-Visible spectroscopy studies. The functionalities present in the sample were studied using FT-IR analysis. The strong band at 3400– 3100  $\text{cm}^{-1}$  which due to either –OH or –NH stretching, a weak band

observed at 2200–2000  $\text{cm}^{-1}$  attributed to the presence of nitrile group, strong absorption band at 1550–1650  $\text{cm}^{-1}$  indicates the presence  $-\text{NH}_2$  group through amide ( $-\text{C}=\text{O}$ ) bonds and the absorption at 1412  $\text{cm}^{-1}$  attributed to the symmetrical deformations of  $\text{CH}_3$  group were in agreement with standard FTIR spectrum of carbon dot. The UV-Visible spectroscopy studies shows the  $\pi \rightarrow \pi^*$  and  $n-\pi^*$  transitions corresponding to  $\text{C}=\text{C}$  and  $\text{C}=\text{O}$  bond which confirms the formation of carbon dot. The TEM studies revealed that the synthesized particles were in the size range of 8-9 nm which confirms the formation of carbon dot and the carbon dots are appreciably spherical and homogeneous. The fluorescence property of the carbon dot was analysed by exciting the particle with UV light and an intense fluorescence were observed at the beginning but the fluorescence stability was weak so the intensity decreases with time.

Zinc oxide and Copper doped Zinc oxide nanoparticles were synthesized via chemical route. Copper was selected as the dopant for our studies due to its unique catalytic and antifungal/antibacterial properties. The synthesized nanoparticles were characterized using XRD, FT-IR, EDAX and SEM studies. The average crystal size was found using XRD studies and it was found to be 13.252 nm for undoped Zinc Oxide and 23.6278 nm for Copper doped Zinc Oxide. In the XRD spectrum an extra peak is observed at  $38.447^\circ$  as compared to undoped Zinc Oxide XRD pattern. This indicates that the copper is doped into the Zinc Oxide lattice. Functional groups were studied using FTIR analysis. The band at 893  $\text{cm}^{-1}$  in copper doped Zinc Oxide nanoparticles was assigned to the vibrational frequencies due to the change in the microstructural features by the addition of Copper into  $\text{Zn}-\text{O}$  lattice. The morphology of synthesized nanoparticles was observed from

SEM studies. There was a remarkable morphology change observed in the shape and particle size of the Copper doped Zinc Oxide nanoparticles which was due to the incorporation of  $\text{Cu}^{2+}$  into  $\text{Zn}^{2+}$  sites. EDAX was used to study the elemental composition of prepared nanoparticles. The EDAX result revealed that the synthesized Copper doped Zinc Oxide Nanoparticles were of high purity, which contain Copper in addition to Zinc and Oxygen of undoped ZnO nanoparticles.

The comparative study of the antibacterial activity of Carbon dot, Carbon dot-Zinc oxide nanocomposite and Copper doped Zinc Oxide-Carbon dot nanocomposite against *E.coli* and *S.aureus* were studied using agar well diffusion method. It has been found that composites exhibit enhanced antibacterial activity than the carbon dot for both the bacterial strains. CD is bacteriosidal against both *E.Coli* and *S.aureus* . CD is showing a zone of inhibition of diameter of 1 cm against both the bacterial strains. For C-dot-ZnO nanocomposite, the diameter of zone of inhibition for *E.coli* became 1.5 cm whereas for *S.aureus* it became 1.2 cm. Cu doped- ZnO-C-dot nanocomposite exhibited enhanced antibacterial activity than both C-dot and C-dot-ZnO nanocomposite. Therefore it can be concluded that the antibacterial activity of C-dot can be enhanced by the preparation of their nanocomposites with ZnO and Cu doped ZnO.

## References

---

### References

1. <https://nexdot.fr/en/history-of-quantum-dots>
2. [https://en.wikipedia.org/wiki/Quantum\\_dot](https://en.wikipedia.org/wiki/Quantum_dot)
3. Anwar Sadat, Haizhen Ding, Mingsheng Xu, Xiaolong Hu, Zhenzhen Li, Jingmin Wang, Li Liu, Lei Jiang, Dong Wang, Chen Dong, Manqing Yan, Qiyang Wang, and Hong Bi, “Recent Advances in Synthesis, Optical Properties, and Biomedical Applications of Carbon Dots.” *ACS Applied Bio Materials* 2(6), P.2317–38, 2019.
4. Bhatia saurabh “Nanoparticles Types, Classification Characterization, Fabrication Methods and Drug Delivery Applications.”, *Natural polymer drug delivery systems*, Springer, P. 33–93, 2016.
5. Bundschuh Mirco, Juliane Filser, Simon Lüderwald, Moira S. McKee, George Metreveli, Gabriele E. Schaumann, Ralf Schulz, and Stephan Wagner, “Nanoparticles in the Environment: Where Do We Come from, Where Do We Go To?”, *Environmental Sciences Europe* 30(1):1–17, 2018.

6. Byrappa K., K. M. Lokanatha Rai, and M. Yoshimura “Hydrothermal Preparation of TiO<sub>2</sub> and Photocatalytic Degradation of Hexachlorocyclohexane and Dichlorodiphenyltrichloromethane.” *Environmental Technology* 21(10):1085–90, 2000.
7. Byrappa, K., and Masahiro Yoshimura, *Handbook of Hydrothermal technology*, William Andrew, 2012.
8. Byrappa Kullaiah, and Tadafumi Adschiri, “Hydrothermal Technology for Nanotechnology”, *Progress in Crystal Growth and Characterization of Materials*, 53(2):117–66, 2007.
9. Das Rashmita, Rajib Bandyopadhyay, and Panchanan Pramanik. 2018. “Carbon Quantum Dots from Natural Resource: A Review.” *Materials Today Chemistry*, 8:96–109, 2018.
10. D’souza, Stephanie L., Shiva Shankaran Chettiar, Janardhan Reddy Koduru, and Suresh Kumar Kailasa, “Synthesis of Fluorescent Carbon Dots Using *Daucus Carota* Subsp. *Sativus* Roots for Mitomycin Drug Delivery.” *Optik* 158:893–900, 2018.
11. Ealia, S. Anu Mary, and M. P. Saravanakumar, “A Review on the Classification, Characterisation, Synthesis of Nanoparticles and Their Application.” *IOP Conference Series: Materials Science and Engineering*, 263:03, 2019.
12. Eckert, Charles A., Barbara L. Knutson, and Pablo G. Debenedetti, “Supercritical Fluids as Solvents for Chemical and Materials Processing.” *Nature*, 383(6598):313–18, 2017.

13. Feng, Xin, Yaoquan Jiang, Jingpeng Zhao, Miao Miao, Shaomei Cao, Jianhui Fang, and Liyi Shi, “Easy Synthesis of Photoluminescent N-Doped Carbon Dots from Winter Melon for Bio-Imaging”, *RSC Advances*, 5(40):31250–54, 2015.
14. Gortari, María Cecilia, and Roque Alberto Hours, “Biotechnological Processes for Chitin Recovery out of Crustacean Waste: A Mini-Review.” *Electronic Journal of Biotechnology*, 16(3):14–14, 2013.
15. U. J. Jing, R. Birringer, U. Gonser, and H. Gleiter. “Investigation of Nanocrystalline Iron Materials by Mössbauer Spectroscopy,” *Applied Physics Letters*, 50(8):472–74, 2000.
16. Hu, Yuefang, Liangliang Zhang, Xuefeng Li, Rongjun Liu, Liyun Lin, and Shulin Zhao, “Green Preparation of S and N Co-Doped Carbon Dots from Water Chestnut and Onion as Well as Their Use as an Fluorescent Probe for the Quantification and Imaging of Coenzyme” *ACS Sustainable Chemistry & Engineering*, 5(6):4992–5000, 2017.
17. Humaera, Nurul Amalia, Ahmad Nurul Fahri, Bidayatul Armynah, and Dahlang Tahir, “Natural Source of Carbon Dots from Part of a Plant and Its Applications: A Review,” *Luminescence* 36(6):1354–64, 2021.
18. Jamkhande, Prasad Govindrao, Namrata W. Ghule, Abdul Haque Bamer, and Mohan G. Kalaskar. 2019. “Metal Nanoparticles Synthesis: An Overview on Methods of Preparation, Advantages and Disadvantages, and Application,” *Journal of Drug Delivery Science and Technology*, 53:101174, 2019.



19. Jelinek, Raz, "Carbon Quantum Dots", *Springer International Publishing, Cham* 29–46, 2017.
20. Khan Ibrahim, Khalid Saeed, and Idrees Khan. 2019. "Nanoparticles: Properties, Applications and Toxicities," *Arabian Journal of Chemistry* 12(7):908–31, 2019.
21. Levy Stuart B and Bonnie Marshall, "Antibacterial Resistance Worldwide: Causes, Challenges and Responses," *Nature Medicine* 10(12):S122–29, 2004
22. Liu Cui, Fang Zhang, Jiao Hu, Wenhui Gao, and Mingzhen Zhang, "A Mini Review on PH-Sensitive Photoluminescence in Carbon Nanodots." *Frontiers in Chemistry*, 1242, 2021.
23. Liu Junjun, Rui Li, and Bai Yang, "Carbon Dots: A New Type of Carbon-Based Nanomaterial with Wide Applications." *ACS Central Science*, 6(12):2179–95, 2020.
24. Liu Wen, Haipeng Diao, Honghong Chang, Haojiang Wang, Tingting Li, and Wenlong Wei, "Green Synthesis of Carbon Dots from Rose-Heart Radish and Application for Fe<sup>3+</sup> Detection and Cell Imaging." *Sensors and Actuators B: Chemical*, 241:190–98, 2017.
25. Liu Yingshuai, Yanan Zhao, and Yuanyuan Zhang, "One-Step Green Synthesized Fluorescent Carbon Nanodots from Bamboo Leaves for Copper (II) Ion Detection." *Sensors and Actuators B:chemical*, 196:647–52, 2014.

- 
26. Mansuriya Bhargav D., and Zeynep Altintas , “Carbon Dots: Classification, Properties, Synthesis, Characterization, and Applications in Health Care—An Updated Review.” *Nanomaterials* 11(10):2525, 2021.
  27. Mourdikoudis, Stefanos, Roger M. Pallares, and Nguyen T. K. Thanh, “Characterization Techniques for Nanoparticles: Comparison and Complementarity upon Studying Nanoparticle Properties.” *Nanoscale*, 10(27):12871–934, 2018.
  28. Muktha, H., R. Sharath, Nagaraju Kottam, S. P. Smrithi, K. Samrat, and P. Ankitha, “Green Synthesis of Carbon Dots and Evaluation of Its Pharmacological Activities.” *BioNanoScience*, 10(3):731–44, 2020.
  29. Muthu Manikandan, Judy Gopal, Sechul Chun, Anna Jacintha Prameela Devadoss, Nazim Hasan, and Iyyakkannu Sivanesan, “Crustacean Waste-Derived Chitosan: Antioxidant Properties and Future Perspective.” *Antioxidants*, 10(2):228, 2021.
  30. Pi Xiaodong, Ting Yu, and Deren Yang, “Water-Dispersible Silicon-Quantum-Dot-Containing Micelles Self-Assembled from an Amphiphilic Polymer.” *Particle & Particle Systems Characterization*, 31(7):751–56, 2014.
  31. Qi Lifeng, and Xiaohu Gao, “Emerging Application of Quantum Dots for Drug Delivery and Therapy.” *Expert Opinion on Drug Delivery* ,5(3):263–67, 2008.

- 
32. Raveendran Varsha, and Renuka Neeroli Kizhakayil “Fluorescent Carbon Dots as Biosensor, Green Reductant, and Biomarker.” *ACS Omega*, 6(36):23475–84, 2021.
  33. Reed M. A, R. T. Bate, K. Bradshaw, W. M. Duncan, W. R. Frensley, J. W. Lee, and H. D. Shih, “Spatial Quantization in GaAs–AlGaAs Multiple Quantum Dots.” *Journal of Vacuum Science & Technology*, 4(1):358–60, 2010.
  34. Sachdev, Abhay, and Packirisamy Gopinath, “Green Synthesis of Multifunctional Carbon Dots from Coriander Leaves and Their Potential Application as Antioxidants, Sensors and Bioimaging Agents.” *Analyst* 140(12):4260–69, 2015.
  35. Sagbas Selin, and Nurettin Sahiner, “Carbon Dots: Preparation, Properties, and Application.” *Nanocarbon and its Composites*. Elsevier, P. 651–76, 2019.
  36. Shi Lihong, Bo Zhao, Xiaofeng Li, Guomei Zhang, Yan Zhang, Chuan Dong, and Shaomin Shuang, “Green-Fluorescent Nitrogen-Doped Carbon Nanodots for Biological Imaging and Paper-Based Sensing.” *Analytical Methods*, 9(14):2197–2204, 2017.
  37. Srivastava, R., S. Majumdar, and S. Bhunia, “Vertically Aligned ZnO Nanorod Grown by Hydrothermal Based Chemical Method on Glass Substrate.” *AIP Conference Proceedings*, Vol. 1447, P. 421–22, 2012.
  38. Sun Xiangcheng, and Yu Lei, “Fluorescent Carbon Dots and Their Sensing Applications.” *TrAC Trends in Analytical Chemistry*, 89:163–80, 2017.

- 
39. Vinoth Kumar, Jothi, Ganesan Kavitha, Rajaram Arulmozhi, Velusamy Arul, Subramanian Singaravadivel, and Natarajan Abirami, “Green Sources Derived Carbon Dots for Multifaceted Applications.” *Journal of Fluorescence*, 31(4):915–32, 2021.
  40. Wang, Ting-Yi, Chong-You Chen, Chang-Ming Wang, Ying Zi Tan, and Wei-Ssu Liao, “Multicolor Functional Carbon Dots via One-Step Refluxing Synthesis.” *ACS Sensors*, 2(3):354–63, 2017.
  41. Wang, Yingte, Xiaoyue Chang, Na Jing, and Yong Zhang, “Hydrothermal Synthesis of Carbon Quantum Dots as Fluorescent Probes for the Sensitive and Rapid Detection of Picric Acid.” *Analytical Methods*, 10(23):2775–84, 2018.
  42. Wang, Youfu, and Aiguo Hu, “Carbon Quantum Dots: Synthesis, Properties and Applications.” *Journal of Materials Chemistry*, 2(34):6921–39, 2014.
  43. Xu, Y., C. Gallert, and J. Winter, “Chitin Purification from Shrimp Wastes by Microbial Deproteination and Decalcification.” *Applied Microbiology and Biotechnology*, 79(4):687–97, 2018.
  44. Yuan, Fanglong, Shuhua Li, Zetan Fan, Xiangyue Meng, Louzhen Fan, and Shihe Yang, “Shining Carbon Dots: Synthesis and Biomedical and Optoelectronic Applications.” *Nano Today* 11(5):565–86, 2016.
  45. Zhang, Ming, Wentao Wang, Ninglin Zhou, Ping Yuan, Yutian Su, Maoni Shao, Cheng Chi, and Feiyan Pan, “Near-Infrared Light Triggered Photo-Therapy, in Combination with Chemotherapy Using

- 
- Magnetofluorescent Carbon Quantum Dots for Effective Cancer Treating.” *Carbon*, 118:752–64, 2017.
46. Zhao, Shaojing, Minhuan Lan, Xiaoyue Zhu, Hongtao Xue, Tsz-Wai Ng, Xiangmin Meng, Chun-Sing Lee, Pengfei Wang, and Wenjun Zhang. 2015. “Green Synthesis of Bifunctional Fluorescent Carbon Dots from Garlic for Cellular Imaging and Free Radical Scavenging.” *ACS Applied Materials & Interfaces*, 7(31):17054–60, 2017.
47. Zhu, Shoujun, Yubin Song, Xiaohuan Zhao, Jieren Shao, Junhu Zhang, and Bai Yang, “The Photoluminescence Mechanism in Carbon Dots (Graphene Quantum Dots, Carbon Nanodots, and Polymer Dots): Current State and Future Perspective.” *Nano Research*, 8(2):355–81, 2015.
48. Das Poushali, Moorthy Maruthapandi, Arumugam Saravanan, Michal Natan, Gila Jacobi, Ehud Banin, and Aharon Gedanken, “Carbon Dots for Heavy-Metal Sensing, PH-Sensitive Cargo Delivery, and Antibacterial Applications.” *ACS Applied Nano Materials* 3(12):11777–90, 2020.
49. Bacon Mitchell, Siobhan J. Bradley, and Thomas Nann, “Graphene Quantum Dots.” *Particle & Particle Systems Characterization*, 31(4):415–28, 2014.
50. Dong Yongqiang, Jianpeng Lin, Yingmei Chen, Fengfu Fu, Yuwu Chi, and Guonan Chen, “Graphene Quantum Dots, Graphene Oxide,

- 
- Carbon Quantum Dots and Graphite Nanocrystals in Coals.” *Nanoscale*, 6(13):7410–15, 2014.
51. Green, Mark “Semiconductor Quantum Dots as Biological Imaging Agents.” *Angewandte Chemie International Edition*, 43(32):4129–31, 2004.
52. Kamat, Prashant V., and Gregory D. Scholes, “Quantum Dots Continue to Shine Brightly.” *The Journal of Physical Chemistry Letters*, 7(3):584–85, 2016.
53. Gao, Dangge, Ping Zhao, Bin Lyu, Yajuan Li, Yelin Hou, and Jianzhong Ma, “Carbon Quantum Dots Decorated on ZnO Nanoparticles: An Efficient Visible-Light Responsive Antibacterial Agents.” *Applied Organometallic Chemistry*, 34(8):e5665, 2020.
54. Gedda, Gangaraju, Chun-Yi Lee, Yu-Chih Lin, and Hui-fen Wu, “Green Synthesis of Carbon Dots from Prawn Shells for Highly Selective and Sensitive Detection of Copper Ions.” *Sensors and Actuators B: Chemical*, 224:396–403, 2016.
55. Ghirardello, Mattia, Javier Ramos-Soriano, and M. Carmen Galan, “Carbon Dots as an Emergent Class of Antimicrobial Agents.” *Nanomaterials*, 11(8):1877, 2021.
56. Guo, Jiazhuang, He Li, Luting Ling, Ge Li, Rui Cheng, Xuan Lu, An-Quan Xie, Qing Li, Cai-Feng Wang, and Su Chen, “Green Synthesis of

- 
- Carbon Dots toward Anti-Counterfeiting.” *ACS Sustainable Chemistry & Engineering*, 8(3):1566–72, 2021.
57. Han Yu, Bijun Tang, Liang Wang, Hong Bao, Yuhao Lu, Cuntai Guan, Liang Zhang, Mengying Le, Zheng Liu, and Minghong Wu, “Machine-Learning-Driven Synthesis of Carbon Dots with Enhanced Quantum Yields.” *ACS Nano*, 14(11):14761–68, 2020.
58. Himaja, A. L., P. S. Karthik, B. Sreedhar, and Surya Prakash Singh, “Synthesis of Carbon Dots from Kitchen Waste: Conversion of Waste to Value Added Product.” *Journal of Fluorescence*, 24(6):1767–73, 2014.
59. Karakoçak, Bedia Begüm, Jue Liang, Shalinee Kavadiya, Mikhail Y. Berezin, Pratim Biswas, and Nathan Ravi, “Optimizing the Synthesis of Red-Emissive Nitrogen-Doped Carbon Dots for Use in Bioimaging.” *ACS Applied Nano Materials*, 1(7):3682–92, 2018.
60. Li, Ning, Zhengtang Liu, Ming Liu, Chaorui Xue, Qing Chang, Huiqi Wang, Ying Li, Zhenchao Song, and Shengliang Hu, “Facile Synthesis of Carbon Dots@2D MoS<sub>2</sub> Heterostructure with Enhanced Photocatalytic Properties,” *Inorganic Chemistry*, 58(9):5746–52, 2019.
61. Liu, Wende, Jinling Liu, Lindsay Triplett, Jan E. Leach, and Guo-Liang Wang, “Novel Insights into Rice Innate Immunity Against Bacterial and Fungal Pathogens.” *Annual Review of Phytopathology*, 52(1):213–41, 2014.

- 
62. Raja, A., S. Ashokkumar, R. Pavithra Marthandam, J. Jayachandiran, Chandra Prasad Khatiwada, K. Kaviyarasu, R. Ganapathi Raman, and M. Swaminathan, "Eco-Friendly Preparation of Zinc Oxide Nanoparticles Using *Tabernaemontana Divaricata* and Its Photocatalytic and Antimicrobial Activity." *Journal of Photochemistry and Photobiology B: Biology* 181:53–58,2018.
63. Ramanan, Vadivel, Senthil Kumar Thiyagarajan, Kaviyaran Raji, Ragupathy Suresh, Rajkumar Sekar, and Perumal Ramamurthy, "Outright Green Synthesis of Fluorescent Carbon Dots from Eutrophic Algal Blooms for In Vitro Imaging." *ACS Sustainable Chemistry & Engineering* ,4(9):4724–31,2021.
64. Reckmeier, Claas J., Julian Schneider, Yuan Xiong, Jonas Häusler, Peter Kasák, Wolfgang Schnick, and Andrey L. Rogach, "Aggregated Molecular Fluorophores in the Ammonothermal Synthesis of Carbon Dots." *Chemistry of Materials*, 29(24):10352–61, 2017.
65. Yang, Jingjing, Xiaodong Zhang, Yong-Hao Ma, Ge Gao, Xiaokai Chen, Hao-Ran Jia, Yan-Hong Li, Zhan Chen, and Fu-Gen Wu. "Carbon Dot-Based Platform for Simultaneous Bacterial Distinguishment and Antibacterial Applications." *ACS Applied Materials & Interfaces*, 8(47):32170–81, 2016
66. Ye, Zhiguo, Guixin Li, Jing Lei, Mei Liu, Yan Jin, and Baoxin Li. "One-Step and One-Precursor Hydrothermal Synthesis of Carbon Dots with



- Superior Antibacterial Activity.” *ACS Applied Bio Materials* 3(10):7095–7102, 2020.
67. Thirukoti Mounika , Shiddappa L Belagali , K.T Vadiraj , “ Synthesis and Characterisation of Zinc Oxide Quantum Dots Using Acidic Precursor” , *Emerging Material Research* , Volume 9 , Issue 2 , P.378-382 , 2020.
68. Thutiyaporn Thiwawong, Korakot Onlaor, Natpasit Chaithanatkun, and Benchapol Tunhoo, “Preparation of copper doped Zinc Oxide nanoparticles by precipitation process for humidity sensing device” , *AIP Conference Proceedings* , Volume 2010, Issue 1 , 2008.
69. Mohammad Shamhari, Boon Siong Wee Suk Fun Chin and Kuan Ying Kok , *Acta Chim* , “ Synthesis and Characterization of Zinc Oxide Nanoparticles with Small Particle Size Distribution” *Chemical and Pharmaceutical Research* , P. 578–585 , 2008.
70. J. Santhoshkumar, S. Venkat Kumar, S. Rajeshkumar , “Synthesis of Zinc Oxide nanoparticles using plant leaf extract against urinary tract infection pathogen”, *Resource-Efficient Technologies*, Volume 3, Issue 4 , P. 459-465 , 2020.
71. S. Radhu, C. Vijayan , “Observation of red emission in wurtzite ZnS nanoparticles and the investigation of phonon modes by Raman spectroscopy”, *Materials Chemistry and Physics*, Volume 129, Issue 3 , P.1132-1137 , 2012.

72. Stefanos Mourdikoudisa, Roger M. Pallares, Nguyen T. K. Thanh, “Characterization Techniques for Nanoparticles: Comparison and Complementarity upon Studying Nanoparticle Properties” , *Nanoscale* , P. 1-8 , 2021.
73. Pawan Sharma & Manish Bhargava, “Applications And Characteris of Nanomaterials In Industrial Environment” , *International Journal of Civil, Structural, Environmental and Infrastructure Engineering Research and Development (IJCSEIERD)* ISSN 2249-6866 Vol. 3, Issue 4, P.63-72 , 2013.
74. Nidhi Raval , Rahul Maheshwari, Dnyaneshwar Kalyane, Susanne R Youngren-Ortiz, Mahavir Chougule, Rakesh Kumar Tekade , “Importance of Physicochemical Characterization of Nanoparticles in Pharmaceutical Product Development” , *Basic Fundamentals of Drug Delivery* , P.369- 400 , 2014.
-